

## MARINE PHOTOSYNTHESIS

### Chapter 2. Optical Properties of the Water Column

by Dale A. Kiefer and Richard J. Collins

The research described in this chapter was performed by the Jet Propulsion Laboratory, California Institute of Technology and by the Department of Biological Sciences of the University of Southern California, under contract with the National Aeronautics and Space Administration.

## Symbols and Definitions (units)

|                   |   |
|-------------------|---|
| $a(\lambda)$      | Absorption coefficient ( $m^{-1}$ ), eqn. 2-5.                                |
| $\kappa^*$        | Diffuse specific absorption coefficient ( $m^{-1} / mg\ CHl\ g$ ), eqn. 2-23. |
| $b(\lambda)$      | Scattering coefficient ( $m^{-1}$ ), eqn. 2-6.                                |
| $c(\lambda)$      | Attenuation coefficient ( $m^{-1}$ ), eqn. 2-12.                              |
| $I_0(\lambda, Z)$ | Scalar irradiance (quanta / $m^2 \cdot sec / nm$ ), eqn. 2-4                  |
| $I_{pan}$         | Photosynthetically Available Irradiance (quanta/ $m^2$ /sec), eqn. 2-3        |
| $I_{pm}$          | Photosynthetically Usable Irradiance (quanta/ $m^2$ /sec), eqn. 2-4.          |
| $k(\lambda)$      | Diffuse Attenuation Coefficient ( $m^{-1}$ ), eqn. 2-18                       |
| $K_{pan}$         | Attenuation Coefficient for $I_{pan}$ , ( $m^{-1}$ ), eqn. 2-21               |
| $K_{pm}$          | Attenuation Coefficient for $I_{pm}$ , ( $m^{-1}$ ).                          |
| $\lambda$         | Wavelength of light, (nm).  |
| $\bar{\mu}$       | Average Cosine of the Irradiance Field, eqn. 2-16.                            |
| $\mu(\lambda, Z)$ | Specific Growth Rate of Phytoplankton, (gm C/gm Chlorophyll/Day)              |
| $\phi(\lambda)$   | Efficiency of Carbon Assimilation, (gmC/quanta absorbed).                     |
| $P^*(\lambda)$    | Primary Productivity, (gm C/ $m^3$ /day), eqn. 2-1                            |
| $Q^*(\lambda)$    | Efficiency Factor for Absorption or Scattering                                |

## Introduction

In this chapter, and in chapter 29, the basic inter-relationship between the flux of radiant energy through the water column and the fixation of carbon by the phytoplankton in the ocean through processes of photosynthesis or primary production will be discussed. The discussions will include the contribution by light scattering and absorption by sea water and biogenic particles to the distribution of radiant energy in the sea that is available for photosynthesis. This discussion will include examples of optical variability in the sea and a consideration of the sources of this variability.

The absorption and scattering of light by phytoplankton represent a significant and sometimes dominant source of light attenuation within the water column. Variations in the concentration of phytoplankton affect both the flux density and spectral composition of light at depth. Since photosynthesis and the growth of phytoplankton is driven by light energy, the vertical distribution of the phytoplankton crop and its production are largely determined by the size and optical properties of the crop itself, and by the vertical distribution of nutrients in the water column. As a result of the attenuation of light by the phytoplankton crop, the radiant energy available to the phytoplankton decreases with depth, often limiting the rates of photosynthesis for intermediate depths. At greater depths, the reduced photon flux is insufficient to support net primary production, and respiration exceeds growth in this portion of the water column.

## Light Absorption and Photosynthesis: The Bio-Optical Model

A simplified conceptual model of the transformations of nitrogen and energy in the planktonic community is illustrated in figure 2-1. These transformations include photosynthetic assimilation of recycled nitrogen in the form of ammonium or urea as well as "new" nitrogen transported by advection or mixing into the euphotic zone from below the seasonal thermocline (Dugdale and Goering, 1969) (see chapter 19). The cellular nitrogen of the phytoplankton crop is eventually transformed by several competing processes. Nitrogen may be recycled, stored in the stock of grazing herbivorous zooplankton, converted into detrital particles by egestion and dissolved organic nitrogen by excretion, transferred to higher trophic levels, or lost from the system by sinking of the crop. If the egested particles are large fecal pellets, they may be rapidly lost from the upper water column by sinking; if small, the particles may remain within the euphotic zone and be subject to photochemical and biological transformations. Particles with diameters less than 20  $\mu\text{m}$  contribute significantly to the absorption and scattering of light in the open ocean. In the illustration shown in figure 2-1, these particles include phytoplankton and suspended material, including detritus, picoplankton, microflagellates, ciliates and cyanobacteria. Although there have been numerous descriptions of these transformations (Cf. Kiefer, 1984), there have been relatively few attempts to formulate the bio-optical properties of the system. To discuss the available energy for the photosynthetic process, we must address the fate of radiant energy as it propagates through the water column and is absorbed or scattered by the seawater, by the marine phytoplankton or other particulate material, or by the dissolved organic material derived from the planktonic community illustrated in figure 2-1.

Figure 2-2 illustrates the partitioning by marine phytoplankton of the absorbed radiant energy into heat, into energy stored within the cell as photosynthetic products and into energy that is re-radiated as fluorescence at longer wavelengths. Energy stored by the cell as heat is lost to the planktonic community as an energy source, but may have a substantial effect on the physical environment of the planktonic community and thus have a direct effect on the productivity of the community. Energy re-radiated by the plankton as fluorescence is substantially lost to the community because the fluorescence band of chlorophyll *a* around 685 nm is in a region in which the absorption coefficient is small for marine phytoplankton (cf. Collins, et al., 1985). Evidence exists (cf. Tophiss and Platt, 1986, Chamberlin, 1989 and Kiefer, et al., 1989) that the amount of energy released by the cell as fluorescence may be related to the photoadaptive state of the plankton and hence may be directly related to the productivity of the cell. The energy stored by the cell as photosynthetic products results in cell growth and division, the primary productivity that insures the propagation of the planktonic community. A further discussion of carbon fixation and partitioning is given in chapter 7.

Ryther and Yentsch (1957) proposed a means of predicting primary production from measurements within the water column of the concentration of chlorophyll *a* and downwelling irradiance. In this work, primary production is estimated by multiplying the concentration of chlorophyll *a* at depth by an empirical factor that is dependent only upon the daily flux of light at that depth. The factor was based on a compilation of field measurements of the assimilation number (photosynthetic rate per unit of chlorophyll *a*) for crops of phytoplankton growing at differing light intensities.

In later work, Platt (1986), Peterson, et al. (1987) and later Platt and Sathyendranath (1988) have proposed that the description of photosynthesis provided by the  $^{14}\text{C}$  method be used to estimate the primary productivity of the planktonic community in terms of the incident irradiance field in the sea. The formulation by Platt and Sathyendranath (1988) utilizes the parameters of the productivity versus irradiance relationship, the biomass normalized initial slope,  $\alpha^B$ , and the biomass normalized maximum photosynthesis,  $P_{\text{m}}^B$ , to describe the primary productivity. This approach uses a generalized biomass profile to describe the variation of the chlorophyll biomass with depth. The irradiance field is computed from the vertical distribution of the chlorophyll biomass. The parameters of the photosynthesis - irradiance relationship are derived from local or regional knowledge based on in situ data.

A mechanistic relationship between marine primary production and the flux of absorbed radiant energy has been described by Kiefer and Mitchell (1983) and by Collins, et al. (1988a) by the equation,

$$P^o(\lambda, z) = \phi(z) a(\lambda, z) F_0(\lambda, z) \quad , \quad (2-1)$$

where  $P^o(\lambda, z)$  is the rate of production in an optically thin suspension of phytoplankton absorbing light at wavelength  $\lambda$ . The absorption coefficient for the cell suspension at that wavelength,  $a(\lambda, z)$ , varies with changes in the size of phytoplankton crop, with the species composition of the phytoplankton and with their photo-adapted and nutrient states. The incident irradiance,  $F_0(\lambda, z)$ , illustrated in figure 2-3, varies with the photon flux density and geometric distribution of light incident upon the sea surface, the rate of attenuation of light with depth caused by absorption and scattering within the water column, and to a lesser extent, on sea state. The product

$a(\lambda, z)I_0(\lambda, z)$  is the flux of absorbed radiant energy through the water column.

The photosynthetic yield,  $\phi(z)$ , expressed as carbon fixed by photosynthesis per photon absorbed, has been formulated by Kiefer and Mitchell (1983) as a function of the incident irradiance. Bidigare, et al. (1987) and Collins, et al. (1988a) have reformulated the photosynthetic yield in terms of the photosynthetically usable irradiance,  $I_{pu}(z)$ , defined in equation 2-4. The maximum photosynthetic yield, at low incident irradiance, appears to be relatively independent of wavelength and species (cf. Morel, 1978), but may vary with nutrient availability and temperature.

Studies of growth and light absorption with continuous cultures of marine phytoplankton have demonstrated that differences in cellular pigment concentration effected by either rates of nutrient supply or photon flux density are closely tied to differences in growth rate. Such observations have prompted Laws and Bannister (1980) and Kiefer and Mitchell (1983) to propose a simple adaptation of equation 2-1 as a formulation of the relationship between specific growth rate and the rate of light absorption by the phytoplankton crop,

$$(\mu + r) = 1/C \phi(z) a_p(\lambda, z) I_0(\lambda, z) \quad (2-2)$$

where  $(\mu + r)$  is the sum of the specific rates of growth,  $\mu$ , respiration,  $r$ , and  $1/C a_p(\lambda, z) I_0(\lambda, z)$  is the rate of cellular light absorption normalized to cellular carbon. The total photosynthetic rate of the cell suspension is obtained by integrating equation 2-1 over the visible spectral region between 400 nm and 700 nm, defined by the absorption by photosynthetic pigments as the region for photosynthetically available radiation.

In the case of light - limited growth, decreases in  $(\mu + r)$  will be accompanied by increases in cellular absorption cross-section. While this formulation is supported by a number of the studies with continuous cultures (c-f. Laws and Bannister, 1980), and is consistent with the model of Ryther and Yentsch (1957), it has not been subjected to either rigorous testing in the field or testing with a number of diverse species of phytoplankton. If this formulation or a similar one is proven correct, the link between the optical properties of seawater and the dynamics of the planktonic community of the upper ocean will be established.

The model described in equation 2-1 was first described by Kiefer and Mitchell (1983) in terms of the photosynthetically available irradiance,  $F_{\text{par}}(z)$ , defined as,

$$F_{\text{par}}(z) = 400 \int^{700} F_0(\lambda, z) d\lambda \quad (2-3)$$

Collins, et al. (1988a) have modified the original model to include the dependence of the photosynthetic yield and the growth and respiration on the photosynthetically usable irradiance,  $F_{\text{pui}}(z)$ , defined by Morel (1978) as the absorbed radiant energy, the product of the spectral absorption coefficient,  $a(\lambda, z)$ , and the scalar irradiance,  $F_0(\lambda, z)$ . Thus,

$$F_{\text{pui}}(z) = 400 \int^{700} \{a_p(\lambda, z)/a_p(435, z)\} F_0(\lambda, z) d\lambda \quad (2-4)$$

where the integrand is the spectral radiant energy absorbed by the phytoplankton.

The model of primary productivity by Collins, et al. (1988a) has been used to compare measured and estimated values of the water - column integrated primary

productivity over large regions of the world's oceans with favorable results. These estimates do not appear to depend on regional or seasonal factors. Using a similar model, Bidigare, et al. (1987) have estimated the vertical distribution of primary productivity in the water column using the absorption coefficients appropriate to the individual pigments, extracted from in situ samples of the phytoplankton population by high-performance liquid chromatography (HPLC) techniques, to define the cellular absorption coefficient.

Although  $E_0(\lambda, z)$  is the primary focus in this chapter, the absorption and scattering properties of the water column,  $a(\lambda, z)$  and  $b(\lambda, z)$ , will be considered in detail because of their primary influence on the structure of the scalar irradiance field in the ocean. Definitions of the optical terms can be found in Jerlov (1976) and in Morel and Smith (1987), and more detailed and comprehensive descriptions of the physics of light transmission on the upper ocean can be found in Jerlov and Nielsen (1974), Preisendorfer (1976), Duntley (1963), Austin and Petzold (1981), Kirk (1986), Siegel and Dickey (1987a,b), Smith and Baker (1978a, b) and Morel, (1988).

### Absorption and Scattering in the Water Column

The propagation of light through the vertical column, as illustrated in figure 2-3, is a complex phenomenon that involves the interaction of two processes, absorption and scattering. Light that is incident on the sea surface comes directly from the sun or from the sky where it has been scattered by the atmosphere. The loss of radiant energy by reflection at the sea surface is small except at low sun angles. The radiant energy entering the water column is attenuated with depth according to the absorption and scattering properties of the water itself and of the suspended and dissolved

n materials, including phytoplankton, picoplankton, bacteria and detrital and dissolved organic material.

The optical properties of the water column may be defined in terms of the inherent optical properties of absorption,  $a(\lambda, z)$ , and scattering,  $b(\lambda, z)$  (cf. Preisendorfer, 1976 and Morel and Prieur, 1977). These properties describe the fractional loss from a unidirectional flux of light by absorption or scattering over a unit distance, and do not depend on the radiance distribution in the water. Each of the inherent optical properties may be described in terms of the individual components of the water column, pure water, the phytoplankton or particulate component and the dissolved component, as

$$a(\lambda, z) = a_w(\lambda) + a_p(\lambda, z) + a_d(\lambda, z) , \quad (?- 5)$$

$$b(\lambda, z) = b_w(\lambda) + b_p(\lambda, z) + b_d(\lambda, z) . \quad (?- 6)$$

Because the particulate and dissolved components vary in concentration throughout the water column, while the contribution by pure water remains constant,  $a(\lambda, z)$  and  $b(\lambda, z)$  vary with depth and cause variations in the submarine light field.

The attenuation of light by absorption is a relatively simple process in which the electromagnetic radiation interacts with absorbing molecules (such as water or pigments) and is converted into other forms of energy as suggested by figure 2-2. Since the flux of light absorbed by water, and by suspended and dissolved materials, varies with wavelength, this process causes changes in the spectral flux density with depth in the submarine light field.

The attenuation of light by scattering is caused by the interaction of electromagnetic radiation with molecules or particles in which both the direction of propagation and the phase of the interacting light may be changed as illustrated in figure 2-3. While this process does not cause a transformation or loss of energy, it does cause changes in the three dimensional distribution of the light field through the processes of Mie and Rayleigh scattering which depend on particle size and index of refraction. The results of both Mie and Rayleigh scattering theory (cf. Born and Wolf, 1965 and van de Hulst, 1983), illustrate that for particle diameters significantly less than the wavelength,  $d \ll \lambda$ , Rayleigh scattering is nearly isotropic. For particles with a diameter greater than the wavelength,  $d \gg \lambda$ , Mie scattering predicts a large forward scattering peak with minimal backward scattering. Scattering in the sea is predominately in small forward angles, a feature that is to be expected if the major contributors to the process are small particles with refractive indices close to that of water. There is a large body of evidence indicating that in open waters, these particles are biogenous, consisting of phytoplankton, detritus, and possibly other components of the microp planktonic community, such as heterotrophic and photosynthetic bacteria, and microzooplankton. These biogenic particles also account for a large amount of the variability in both the absorption coefficient,  $a(\lambda, z)$ , and the scattering coefficient  $b(\lambda, z)$ . The upwelled radiance,  $I_u(\lambda)$ , illustrated in figure 2-3 results from the backward scattering from these small particles in the sea.

Scattering by marine particles disperses the light field, increasing the probability of absorption of a photon by increasing the mean optical pathlength over a geometric depth interval. In an optically homogenous medium, the diffuse nature of the light field increases with depth until an asymptotic isotropic distribution is reached and the radiance distribution remains constant with increasing depth (cf. Kirk, 1986).

Since scattering by suspended materials varies with wavelength and particle size, this process, like absorption, causes variations in the spectral distribution of the submarine light field.

### **Optical Properties of Pure Water**

The absorption coefficient for pure sea water,  $a_w(\lambda)$ , has been described by Morel and Prieur (1977) and is shown in figure 2-4 as a function of the wavelength. This spectrum is characterized by larger values in the red portion of the spectrum than in the blue, and a minimal value near 465 nm. In contrast, an absorption coefficient characteristic of dissolved organic material,  $a_d(\lambda)$ , also described by Morel and Prieur (1977), is characterized by larger values in the blue portion of the spectrum than in the red, as illustrated in the same figure. The total absorption coefficient,  $a(\lambda)$ , given by equation 2-5, is shown in figure 2-4.

The Rayleigh scattering of light by water molecules contributes nearly equal amounts to the forward and backward components of the scattering,  $b_w(\lambda)$ . As shown in figure 2-4, the value for the scattering coefficient for water varies little over the visible region of the spectrum. The combined effects of minimal absorption in the blue region and spectrally independent scattering cause pure water to act as a broad-band blue filter. With increasing depth, red, yellow, green and finally the shorter wavelengths of blue light are sequentially removed until the spectral region near 465 nm predominates.

## Optical Properties of Biogenous Particles

in waters free of terrestrial or fluvial influence, the major sources of optical variability are the Concentration of phytoplankton and associated detrital particles which may vary by over three orders of magnitude in coastal and open waters. At higher concentrations, these particles dominate the absorption and scattering within the water column. For phytoplankton, most of the absorption is by the photosynthetic and photoprotective pigments found within the chloroplast. For detritus, absorption is caused by these same pigments and their degraded forms.

Measurements of the spectral absorption properties of marine particles have been obtained by spectrophotometric techniques (Yentsch, 1967, Kiefer and SooHoo, 1982 and Kishino, et al., 1984). Figure 2-5 is an example of the vertical distribution of the mean value of the spectral absorption coefficient for phytoplankton,  $a_p(z)$ , obtained on the Biowatt 11 cruise in August, 1987 at a station in the southern Sargasso Sea. These data from Chamberlin (1989) represent the mean value of the spectral absorption coefficient, formed by the integral over wavelength of the spectral distribution for the chlorophyll *a* specific absorption coefficient shown in figure 2-6, and indicate a strong sub-surface maximum in the mean absorption coefficient caused by an increase in pigment concentration per cell at low light levels. The spectra of  $a^*(\lambda, z)$ , shown in figure 2-6, taken from the work of Chamberlin (1989), indicate that the photosynthetic pigments are a major source of particle absorption and provides information about the concentration of pigments per cell as well as the concentration of detrital material. In figure 2-6, the red absorption band of chlorophyll *a*, centered at 676 nm, and the Soret bands of chlorophyll *a* centered at 436 nm, and those of phaeophytin *a* centered near 418 nm, reflect the summed concentrations of chlorophyll

a and phaeophytin a. Derivatives of the absorption coefficient with respect to wavelength, shown in figure 2-7 from the work of Morrow (1989), have been used to estimate concentrations of chlorophyll a, b, and c (Faust and Norris 1982, Bidigare, et al., 1988 and Morrow, 1988). The top panel of figure 2-7 illustrates a representative phytoplankton absorption coefficient spectrum. The lower panel illustrates the results of a fourth -derivative analysis which exhibits several of the principal cellular pigment components. Verification of pigment identification using high performance liquid chromatography (Bidigare, et al., 1988) has permitted the use of derivative techniques in this analysis of in situ spectral data.

The general flatness of the spectra and the enhanced absorption in the blue region of these spectra relative to that in the red when compared to laboratory cultures, indicates that detrital pigments are also important contributors to absorption in the sea. The relative contributions of the phytoplankton and detrital components to the particulate absorption spectra have been studied using multiple regression analysis to decompose the spectra. This technique is illustrated by the work of Morrow, et al. (1989) shown in figure 2-8. Figure 2-8a shows the spectral distribution of the total particulate absorption spectrum together with the derived component spectra. Figure 2-8b illustrates the regression between the chlorophyll a concentration and the particulate absorption at 440nm. The open circles represent the total  $a_p(440)$  and the filled triangles represent the decomposition to the phytoplankton component. This technique has been successfully demonstrated to provide a measure of the detrital fraction from in situ samples.

Analysis of field data indicates that absorption coefficient spectra,  $a_p(\lambda, z)$ , from particles collected from the upper **mixed** layer and from below the chlorophyll

maximum most often appear to be enriched in detrital pigments, while spectra from particles collected from waters of intermediate depths suggest lower contributions from detritus. It is possible that the increased amount of detrital pigments within the mixed layer relative to intermediate depths is caused by higher rates of production of small detrital particles by microzooplankton. The detrital pigments produced by grazing, including phaeophytin *a* and phaeophorbide *a*, may be further altered by photo-oxidation. In the aphotic zone, where there is no local production by phytoplankton, detrital pigments must be supplied by egestion of vertically migrating herbivores, or the breakdown of sinking fecal pellets.

The absorption coefficient for a suspension of particles of uniform size and optical properties, may be described in terms of the efficiency factor for particulate absorption,  $Q_a^i(\lambda)$ , as,

$$a_p^i(\lambda) = N^i G^i Q_a^i(\lambda) \quad , \quad (2-7)$$

where  $N^i$  is the concentration of the particles in the suspension and  $G^i$  is the geometrical cross-section of the individual particle. The product  $N^i G^i$  is the fraction of the incident light beam that is intercepted by the particle suspension over a unit path length. The efficiency factor for particulate absorption,  $Q_a^i(\lambda)$ , is defined as the fraction of light incident upon the particle that is absorbed by the pigments contained in the particle. For the case of a spherical particle of uniform pigment concentration,  $Q_a^i(\lambda)$ , is a function of the parameter  $\rho(\lambda) = a_{cm}(\lambda)d$ , the optical density of the particle along the central ray, where  $a_{cm}(\lambda)$ , the absorption coefficient for the cellular pigments (cf. van de Hulst, 1983), is related to the imaginary part of the refractive index, and is a function of both the concentration of pigments within

the particle and the molecular absorption cross-sections of the pigments. The behavior of the efficiency factor for particulate absorption, is illustrated in figure 2-9, where  $Q_a^i(\lambda)$  is shown as a function of  $\rho(\lambda)$ . The values of  $Q_a^i(\lambda)$  range between 0 for a nonabsorbing particle and 1 for a particle that absorbs all light that it intercepts. As  $Q_a^i(\lambda)$  increases, the absorption spectrum tends toward a white spectrum as discussed by Morel and Bricaud (1981), Bricaud, Morel and Prieur (1983) and Collins, et al. (1985).

The scattering coefficient for a Suspension of particles of uniform size and optical properties, may be described in terms of the efficiency factor for particulate scattering,  $Q_b^i(\lambda)$ , according to the expression,

$$b_p^i(\lambda) = N^i G^i Q_b^i(\lambda) \quad , \quad (?-8)$$

where the efficiency factor for scattering,  $Q_b^i(\lambda)$ , is defined as the fraction of the flux of light incident on the particle that is scattered. This factor is the difference between the efficiency factor for attenuation and the factor for absorption,  $Q_b^i(\lambda) = Q_{atten}^i(\lambda) - Q_a^i(\lambda)$  and may be calculated from Mie scattering theory (cf. van de Hulst, 1983, Born and Wolf, 1965 and Kirk, 1986) as a function of the phase shift of light propagating along the central ray of the particle,  $\rho(\lambda)$ , defined in terms of the particle size and the real and imaginary parts of the refractive index.

Figure 2-9 shows the behavior of  $Q_{atten}^i(\lambda)$ , the efficiency factor for the attenuation of a beam of light through processes of absorption and scattering by particles. For nonabsorbing spheres this factor becomes the efficiency factor for

scattering,  $Q_b^i(\lambda)$ . For particles that are small or have indices of refraction that are close to that of water, the phase shift is small, and  $Q_b^i(\lambda)$  approaches 0. For increasing values of  $\rho(\lambda)$ ,  $Q_b^i(\lambda)$  asymptotically approaches the value of 2 indicated in figure 2-9. The oscillations in  $Q_b^i(\lambda)$  result from the scattering of light into small forward angles by interference and diffraction. Since the relative refractive index of marine phytoplankton cells has been found to be in the range of 1.03 to 1.15, one can estimate the efficiency with which biogenous particles of differing sizes scatter light by estimating the value of  $\rho(\lambda)$  (cf. Bricaud, Morel and Prieur, 1983).

In seawater, the suspended particles are a diverse assemblage of planktonic and bacterial species, detritus and inorganic material. The contribution of this assemblage to the absorption of the medium is represented by the sum over all particles of the products shown in equation 2-7,

$$a_p(\lambda) = \sum_i N^i G^i Q_a^i(\lambda) \quad (2-9)$$

Variations in  $a_p(\lambda)$  are caused by changes in either the geometric cross-section of the particulate suspension, ( $N^i G^i$ ), or in the optical efficiency factor for absorption,  $Q_a^i(\lambda)$ , because of variations in the pigment concentration. For phytoplankton, the cellular concentrations of pigment may vary as a consequence of photoadaptation and nutrient supply. The variation in cellular pigment concentration with cellular diameter is shown in figure 2-10 from the work of Morrow (1988). This figure illustrates the importance of the increased pigment density, and hence  $a_{cm}$ , for smaller cells and their relative contribution to the absorption properties of the water column. Because of the considerable diversity of marine particles and the corresponding difficulty of examining individual marine particles (cf. Iturriaga, et al., 1988 and

Morrow, et al., 1989), application of equations 2-7 and 2-8 to marine optics have been very limited.

Measurements with electronic particle counters shown in figure 2-11 (cf. Zaneveld and Pak, 1979) illustrate that for the upper waters of relatively large geographic regions, the particle size distribution remains relatively constant, with the numerical concentration,  $N^i$ , of particles of a given diameter,  $d_i$ , increasing with decreasing diameter according to,

$$N^i(d_j) = A (d_j)^{-B} . \quad (2-10)$$

In this formulation,  $A$  and  $B$  are empirical constants. For particles larger than  $1 \mu\text{m}$  in equivalent diameter, values for the total particle load, represented by  $A$  in equation 2--10, vary by over an order of magnitude while the values for the slope,  $B$ , remain relatively constant between 3.5 to 5 with most values close to 4. Because the value of the geometric cross section of a particle,  $G^i$ , increases as the square of the diameter and the concentration of particles,  $N^i$ , decreases as the inverse fourth power ( $B=4$ ), the fraction of light intercepted by particles of a given diameter, ( $N^i G^i$ ) will increase, for decreasing particle size, as the inverse second power of the particle diameter. Thus, as the particle diameter decreases, ( $N^i G^i$ ) increases together with an increase in pigment density, as illustrated in figure 2- 10. Therefore, particles with diameters less than  $20 \mu\text{m}$  are often the major contributors to the absorption and scattering of light in seawater.

## Beam attenuation

The difficulty of measuring the inherent optical properties of seawater occurs in part because of multiple scattering of photons. These problems can be circumvented with a submersible transmissometer (cf. Bartz, Zaneveld and Pak, 1978), an instrument designed to measure the loss of light from a collimated beam. The Lambert-Beer Law is used to calculate the beam attenuation,  $c(\lambda, z)$ , the inherent optical property that describes the fractional losses of a beam of light as it traverses a unit distance (cf. figure 2-3), as,

$$c(\lambda, z) = \exp \{ -T(\lambda, z) \} , \quad (2-11)$$

where  $T(\lambda, z)$  is the transmittance of the beam of light at a specific wavelength, calculated as the ratio of the detected to the incident radiance, over a specific path length. Because losses from the beam are the result of absorption and scattering, these losses may be described as the sum,

$$c(\lambda, z) = a(\lambda, z) + b(\lambda, z) . \quad (2-12)$$

In terms of the efficiency factor for attenuation described previously, the beam attenuation coefficient for an assemblage of particles becomes,

$$c_p(\lambda) = \sum_i \{ N^i G^i Q_{\text{atten}}^i(\lambda) \} . \quad (2-13)$$

At appropriate wavelengths, the beam attenuation coefficient,  $c(\lambda, z)$ , has been found to covary with the concentration of particles in the sea. Figure 2-12

illustrates the dependence of the particulate concentration on the beam attenuation coefficient,  $c(665)$ , for samples at various depths within the euphotic zone at a number of stations in the northeastern Pacific. The covariation observed indicates that both the distribution of particle sizes,  $G^i$ , and the efficiency factor for beam attenuation,  $Q_{atten}^i(\lambda)$ , do not vary significantly over this geographic region, and therefore the value of the beam attenuation coefficient provides a good measure of particle load or particle concentration,  $N^i$ , as illustrated in the figure.

Studies of the relationship between  $c(\lambda, z)$  and in situ fluorescence of chlorophyll *a* in the upper water column (Kiefer and Austin, 1974 and Lieberman et al., 1984) have shown a general covariance of  $c(660, z)$  with chlorophyll *a* concentration as illustrated in figure 2-13. A closer examination of the variance in the relationship between the concentration of chlorophyll *a* and the value of  $c(660, z)$  in figure 2-13 indicates that values of the ratio  $c(660, z) / \text{chlorophyll } a$  tend to decrease with depth because of photoadaptation of phytoplankton. Figure 2-14 illustrates the ratio of  $c(660, z) / \text{chlorophyll } a$  plotted by Kiefer (1984) as a function of the optical depth for measurements made in the northeastern Pacific. Within the depth profile of a single station, three distinct depth intervals are apparent. In the uppermost part of the water column, illustrated as region 1 in figure 2-13, values for the ratio are maximal and constant, as illustrated by the constant values shown in figure 2-14. This is the depth interval of the upper mixed layer where light levels are highest, and the absorption coefficient of the particles is smallest relative to their scattering coefficient. In the depth interval below the mixed layer, increasing depth leads to large increases in the absorption coefficient of the particles relative to their scattering coefficient, causing a decrease in the ratio  $c(660, z) / \text{chlorophyll } a$ . This region of change in the optical properties of the particles, shown as region 3 in

figure 2-13, extends to the bottom of the euphotic zone,  $K_{par}Z_e = 4.6$ . Unlike the mixed layer, rates of vertical mixing appear to be sufficiently slow below the euphotic zone that the ratio remains relatively constant with depth, leading to region 4 in figure 2-13. This pattern is remarkably similar for coastal and open ocean stations in the northeastern Pacific and is most simply explained by increases in the pigment concentration of phytoplankton growing at lower light levels. Within the mixed layer rates of vertical mixing may be more rapid than rates of photoadaptation so that the optical properties of the cells and associated detritus are uniform within the layer. Below the mixed layer, rates of vertical mixing may be slower than rates of photoadaptation, and at the bottom of the euphotic zone, low light adaptation is complete and further increases in the cellular concentration of chlorophyll *a* with depth may not occur.

#### The Scalar Irradiance Field

Combining the processes of absorption and scattering, the exponential nature of light attenuation within the water column is described by the Lambert-Beer Law,

$$E_o(\lambda, z+dz) = E_o(\lambda, z) \exp - \left\{ \int_z^{z+dz} k(\lambda, \xi) d\xi \right\}, \quad (2-14)$$

where,  $E_o(\lambda, z)$  is the spectral scalar irradiance measured with a spherical collector.  $k(\lambda, z)$ , the attenuation coefficient for diffuse irradiance between depths  $z$  and  $z+dz$ , is an apparent optical property of the water because its value depends on the absorption and scattering properties of the seawater and on the radiance distribution of the light field (Preisendorfer, 1976).

A more useful description of the scalar irradiance field at depth can be derived from the Gershun equation describing the downwelling irradiance,  $E_d(\lambda, z)$  (cf. Kirk, 1986),

$$E_d(\lambda, z+dz) = E_d(\lambda, z) \exp - \left\{ \int_z^{z+dz} a(\lambda, \xi) / \bar{\mu}_d(\lambda, \xi) d\xi \right\} , \quad (2-15)$$

where  $E_d(\lambda, z)$  is defined as the light vector normal to the ocean surface which incorporates all light propagating downward from the sea surface. It is this light field that is normally measured by optical instruments in the sea. The behavior of the downwelling irradiance field with depth is illustrated in figure 2-15. In figure 2-15a, the vertical profiles of the photosynthetically available irradiance,  $E_{par}(z)$  are illustrated for uniform concentrations of pigment throughout the euphotic zone. In figure 2-15b, the spectral dependence of the downwelling irradiance is illustrated for Jerlov Case I waters with a pigment concentration of  $5 \mu\text{g/l}$ , demonstrating the exponential nature of the spectral irradiance for uniform pigment concentration.

In equation 2-15,  $\bar{\mu}_d(\lambda, z)$ , is the average cosine of the downwelling irradiance field, a dimensionless parameter that describes the effects of changes in the three dimensional distribution of radiance at depth, defined as,

$$\bar{\mu}_d(\lambda, z) = E_d(\lambda, z) / E_{0d}(\lambda, z) , \quad (2-16)$$

the ratio of the downwelling irradiance,  $E_d(\lambda, z)$  to the downwelling scalar irradiance,  $E_{0d}(\lambda, z)$ . The reciprocal of the average cosine,  $\bar{\mu}_d(\lambda, z)^{-1}$ , is equal to the mean pathlength a photon travels over a unit distance normal to the sea surface. The Gershun approximation permits the description of the inverse of the average cosine of

the scalar irradiance field as,

$$\overline{\mu_d(\lambda,z)}^{-1} = k_d(\lambda,z) / a(\lambda,z) . \quad (2-17)$$

Measurements of the average cosine of the scalar irradiance field at a given wavelength indicate that its value undergoes relatively small changes with depth as indicated in figure 2-16, where the average cosine for the total irradiance and for the downwelling irradiance are plotted as a function of the optical depth for the downwelling irradiance field.

The attenuation coefficient for the scalar irradiance,

$$k(\lambda,z) = 1 / E_0(\lambda,z) dE_0(\lambda,z) / dz , \quad (2-18)$$

is an apparent optical property of the medium, depending in part on the diffuse nature of the light field (cf. Baker and Smith, 1982, Kirk, 1956, Siegel and Dickey, 1987a,b and Morel, 1988), but is determined largely by the composition and concentration of material in seawater. As an increased number of field measurements of spectral irradiance have been obtained, the spectral character of the relationship between photosynthetic pigment concentration and  $k(\lambda,z)$  has been better defined. Morel and Prieur (1977), Smith and Baker (1978a), Baker and Smith (1982) and Prieur and Sathyendranath (1981) have all described the contributions to the spectrum of  $k(\lambda,z)$  from pure sea water, the biogenous components, particulate detrital material and dissolved organic compounds in the sea. Although not rigorous, the diffuse attenuation coefficient,  $k(\lambda,z)$ , may be attributed with quasi-inherent optical properties (cf. Preisendorfer, 1976) because of the weak dependence on the geometric distribution of

the irradiance field, and may be represented by the sum,

$$k(\lambda, z) = k_w(\lambda, z) + k_p(\lambda, z) + k_d(\lambda, z) \quad (2-19)$$

The diffuse attenuation coefficient for pure water,  $k_w(\lambda)$ , derived from the data of Baker and Smith (1982), is shown in figure 2-17 in comparison to the value of  $k_p(\lambda)$  for particulate material. In this figure,  $k_p(\lambda, z)$ , derived from Morel (1988) and described in equation 2-20, is characterized by a red attenuation band for chlorophyll *a* and a broad blue attenuation contributed by the superpositioning of the Soret bands of chlorophyll *a* with bands for the accessory chlorophylls and carotenoids.

Austin and Petzold (1981, 1984), Baker and Smith (1979, 1982) and Morel (1988) have described the diffuse attenuation coefficient,  $k(\lambda, z)$ , in terms of the coefficient at a particular wavelength,  $k(490, z)$ , or in terms of the pigment concentration in the water. In the latest of these papers, Morel (1988) has described the spectral diffuse attenuation coefficient by the equation,

$$k(\lambda, z) = k_w(\lambda) + \chi(\lambda) C(z)e^{k(490, z)z} \quad (2-20)$$

where  $C(z)$  is the pigment concentration at depth  $z$ , including both the chlorophyll *a* and the phaeopigments at that depth. From this equation, and from knowledge of the pigment composition of the water column, the scalar irradiance field may be estimated using equation 2-14 or 2-15. Figure 2-18 illustrates the behavior of the diffuse attenuation coefficient at a number of wavelengths as a function of the pigment concentration from equation 2-20,

Morel and Prieur (1977) found it necessary to define two water color types: those characteristic of the open ocean, in the absence of terrigenous particles, for which biogenous particles were the dominant source of optical variability and  $k_d(\lambda, z)$  does not contribute significantly to equation 2-19, and those for which inorganic particles were dominant, presumably because of significant input of terrigenous or lacustrine materials. The behavior of  $k_d(\lambda, z)$ , not illustrated in figure 2-17, is often characterized by the continual rise in attenuation in the blue region of the spectrum for these latter regions.

The integral of equation 2-14 is the photosynthetically available radiance,  $E_{par}(z)$ , given by equation 2-3. From this equation the diffuse attenuation coefficient for the photosynthetically available radiation,  $K_{par}(z)$ , may be calculated according to the equation,

$$K_{par}(z) = 1 / E_{par}(z) \ d E_{par}(z) / dz . \quad (2-2'1)$$

The results of the calculation of  $K_{par}(z)$  are shown in figure 2-19 for fixed values of the ratio of the photosynthetically available radiance,  $E_{par}(z)$ , to its surface value and for increasing pigment content. Figure 2-19 illustrates that  $K_{par}(z)$  is a function both of pigment concentration and the depth within the euphotic layer. This fact is responsible for the curvature of the vertical profiles of  $E_{par}(z)$  shown in figure 2-15a. This figure demonstrates that the diffuse attenuation coefficient for photosynthetically available radiation is not a constant with depth even for a vertically uniform pigment field, but varies significantly near the surface, becoming asymptotically uniform with increasing depth.

In equation 2-19 and in equations 2-5 and 2-6, the particulate and dissolved components may be represented as the product of the chlorophyll a specific coefficient and the chlorophyll a concentration. Thus, the chlorophyll a specific absorption coefficient,  $a^*(\lambda, z)$ , may be described as,

$$a(\lambda, z) = a^*(\lambda, z) \langle \text{Chl } \underline{a} \rangle \quad , \quad (2-22)$$

where the value of  $\langle \text{Chl } \underline{a} \rangle$  is the concentration of chlorophyll a in the suspension.

Using the results of equations 2-3 and 2-4, an effective absorption coefficient for phytoplankton, " $a^*(z)$ ", can be defined that is a measure of the absorption by phytoplankton of the radiant energy available in the photosynthetic wavelength band. This coefficient is defined by the relationship,

$$a^*(z) = \frac{\int_{400}^{700} a^*(\lambda, z) E_0(\lambda, z) d\lambda}{\int_{400}^{700} E_0(\lambda, z) d\lambda} \quad , \quad (2-23)$$

or

$$a^*(z) = \frac{a^*(435, z) E_{\text{pur}}}{E_{\text{par}}} \quad , \quad (2-24)$$

the ratio of the photosynthetically usable radiance to the photosynthetically available radiance. The behavior of  $E_{\text{pur}}(z)$  has been described by Morel (1978) and by Collins, et al. (1988b) and is illustrated in figure 2-20 as a function of the photosynthetically available radiance,  $E_{\text{par}}(z)$ . This figure illustrates that the effective absorption coefficient is a function of the pigment concentration because of the effect of pigment on the scalar irradiance field.

The variation of the spectral downwelling irradiance field with increasing pigment concentration and depth is caused by the variations in the spectral distribution of  $k_d(\lambda, z)$  illustrated in figure 2-17 and equation 2-19. The downwelling irradiance field that results from including both sea water and biogenous particles in the computation of the diffuse attenuation coefficient as a function of depth is illustrated in figure 2-21. Figure 2-21a, which illustrates the vertical distribution of the downwelling irradiance for pure sea water, indicates the strong absorption in the red portion of the spectrum. Figure 2-21b illustrates the spectral narrowing caused by a uniform pigment concentration of  $5 \mu\text{g/l}$ . The photosynthetically usable irradiance defined by equation 2-4 is the product of the spectral absorption coefficient illustrated in figure 2-4 and the scalar irradiance, which exhibits a spectral narrowing similar to that shown in figure 2-21b for the downwelling irradiance. The ratio of these two fields is the average cosine shown in figure 2-16. These computations illustrate the enhanced blue absorption caused by chlorophyll  $a$ .

The intensity of the scalar irradiance field in the ocean has been shown to be determined to a great extent by the phytoplankton population. One measure of the extent of the scalar irradiance field is the euphotic depth,  $Z_e$ , defined as the depth for which the photosynthetically available radiance,  $F_{\text{par}}$ , is 1% of its value at the surface.  $Z_e$  is a practical measure of the depth to which light will penetrate in the ocean and has often been approximated by the use of the Secchi disk. For the purpose of evaluating the primary productivity in the ocean, a more realistic measure might be the depth for which the photosynthetically usable radiance,  $F_{\text{pur}}$ , is 1% of the value at the surface. This depth will depend both on the pigment concentration and to a limited extent on the time of day because the spectrum of the irradiance field at the surface is a function of the solar ephemeris.

## Patterns in Vertical Distributions

While our present understanding of the causes of optical variability in the sea is incomplete, the increased number of biological and optical measurements made in recent years has led to significant advances. Our understanding of the changes that occur within the water column are based upon the observation of similar patterns of vertical distribution of biological and optical parameters at different geographic regions and their explanation by the relationships described above, Figure 2-22 (cf. Siegel and Dickey, 1987a), illustrates the patterns obtained in October, 1982 from the ODFX cruise in the northeastern Pacific Ocean. At this station, there exists a well-mixed surface layer in which the temperature is invariant with depth over the upper 50 m of the water column. The seasonal thermocline appears to extend from 50 m to 80 m. Nitrate levels are at the limit of detectability within the surface mixed layer and the upper part of the seasonal thermocline. However, at 90 m, below the permanent thermocline, nitrate concentrations begin to increase rapidly with increased depth.

Figure 2-22a shows the vertical distribution of chlorophyll *a*, chlorophyll *a* fluorescence, the potential density and the beam attenuation coefficient,  $c(660)$  at this station. The concentration of chlorophyll *a*, as estimated from fluorescence, remains relatively constant in the surface mixed layer to 50 m, increasing below this layer, and continuing to rise to 90 m. Below this depth, the concentration of chlorophyll *a* decreases at first rapidly to 120 m and then more slowly. The distribution of the beam attenuation coefficient, a measure of particle concentration, while constant in the surface mixed layer, exhibits a deep maximum at 70 m, above the chlorophyll maximum. Below the depth of the chlorophyll maximum, the vertical

distribution of beam attenuation closely resembles that of chlorophyll *a*, decreasing rapidly to 120 m and more slowly below.

Figure 2-22b illustrates the vertical distribution of the spectral diffuse attenuation coefficient in the water,  $k_d(\lambda)$ , for different wavelengths in the visible portion of the spectrum. The diffuse attenuation coefficient for the particulate material in the water,  $k_p(\lambda) = k_d(\lambda) - k_w(\lambda)$ , the difference between the total diffuse attenuation coefficient and the diffuse attenuation coefficient for water, most closely resembles the distribution of chlorophyll *a* in the mixed layer as shown in figure 2-22a.

The patterns described in figure 2-22 are characteristic of oceanographic regions where the upper water column contains a well-defined surface mixed layer and a well developed or stable pycnocline. These patterns will be particularly well-defined in regions where nutrient concentrations are low within the surface mixed layer and upper parts of the seasonal mixed layer. Such conditions prevail in much of the world's oceans and offshore waters. The major exceptions to this statement are regions of active upwelling, deep or rapid vertical mixing, or where the standing crop of phytoplankton is dominated by large motile species such as the dinoflagellates. A reasonable interpretation of the patterns shown in figure 2-22 requires a description of the coupling between the physical and biological properties of the ocean. The chlorophyll maximum appears at 90 m, at the bottom of the euphotic zone. In overlying waters, decreases in chlorophyll *a* concentration are caused primarily by the adaptation of the phytoplankton to higher light levels and to lower concentrations of nutrients. This interpretation is supported by the fact that the beam attenuation coefficient, a measure of particle concentration, does not decrease significantly in the waters above

90 m. The constant value for both the beam attenuation coefficient and chlorophyll *a* concentration within the surface mixed layer results from the fact that vertical mixing within the layer is sufficiently rapid to eliminate changes caused by differences in either adaptation or net growth at different depths within the layer. Between the surface mixed layer and the chlorophyll maximum, rates of vertical mixing are slow enough so that such differences between depths caused by local adaptation and net production are expressed in the profiles for chlorophyll *a* and beam attenuation.

Below the chlorophyll maximum, the intensity of the scalar irradiance,  $F_0(\lambda, z)$ , is sufficiently low that the local gross primary production,  $P^g(\lambda)$ , given by equation 2-1 is equal to or less than respiration by the phytoplankton. The depth for which the local production equals respiration has been defined by Sverdrup, (1953) as the critical depth. Below the critical depth, respiration exceeds growth. At these depths, for which the light is less than 1% of the surface irradiance, a level defining the depth of the euphotic zone, the cells are optimally adapted for low light conditions as mixing does not occur with the surface waters and their relatively intense scalar irradiance. Thus, there are no further increases in the cellular concentration of pigments in the underlying waters. These waters immediately below the chlorophyll maximum are characterized by vertical patterns in which decreases in the beam attenuation coefficient are mirrored by decreases in the chlorophyll *a* concentration, and increases in nutrient concentration, because the cells can not utilize nutrients effectively. In this water, vertical eddy transport between the particle-enriched water of the lower euphotic zone and the deeper, particle-free water is now dominant.

## Relationships to Remote Sensing

The relationship between the spectral distribution of the upwelling radiance,  $I$ ,  $U(A)$ , or the water color, and the optical properties of the water are used in the remote sensing of the biomass and primary productivity of the ocean through the description of the remote sensing reflectance,  $R(\lambda)$ , described in detail in chapter 28. Morel and Prieur (1977) and Smith and Baker (1978b) described the remote sensing reflectance as,

$$R(\lambda) = 1/3 \ b_b(\lambda) / a(\lambda) \quad . \quad (2-25)$$

Because both the backscatter and the absorption are functions of the biogenous particulate load in the water column, the remote sensing reflectance is dominated by the concentration of phytoplankton in the water. The consequences of this fact for the remote sensing of phytoplankton biomass through pigment analysis, and of the estimate of primary productivity of the phytoplankton crop will be explored in Chapter 28.

## Future Research

There are many unanswered questions in the relatively new field of marine biological optics; a few examples are listed below:

1. What particles in seawater contribute to the absorption and scattering of light? Are cyanococoid bacteria important contributors to optical properties? How important are detrital particles and heterotrophic bacteria? Methods such as flow cytometry and microphotometry that are capable of determining the optical properties of individual particles may help provide answers to these questions.
2. More must be learned about the quantum yield of photosynthesis,  $\phi(z)$ , since this parameter is the critical link between light absorption and primary production. Is this parameter only a function of photon flux density and independent of phytoplankton species, nutrient availability, or temperature? If not, what is its dependence upon these ecological and species-dependent parameters?
3. Present understanding of the absorption properties of marine particles is far from complete. There have been almost no attempts to identify the photosynthetic accessory pigments or photo-protective pigments that contribute to the absorption coefficient. Application of HPLC to field studies is just beginning, and rapid progress in pigment identification is soon expected. This question may include a consideration of the effects of phytoplanktonic species succession upon the optical properties of the particles or the seawater itself.
4. The optical properties of dissolved organic material have been neglected in this

chapter. More needs to be learned about its contribution to light absorption, its distribution, and its origin and fate.

5. Recent studies with submersible spectroradiometers have shown that the attenuation with depth of red light around 680 nm is not consistent with the Lambert-Beer Law. Light levels within the euphotic zone are much higher than would be expected from the diffuse attenuation expected for both water and the concentration of chlorophyll *a*. The anomalously high levels of red light appears most likely to be caused by the "natural" or solar induced fluorescence of chlorophyll *a* within the phytoplankton cells. Can this signal provide valuable information about the size of the phytoplankton crop or perhaps even information about the crop's rate of light absorption or rate of primary production?

## References

Austin, R.W. and T.J. Petzold, 1981: The Determination of the Diffuse Attenuation Coefficient of Sea Water Using the Coastal Zone Color Scanner. *Oceanography from Space*, J.F.R. Gower ed., Plenum Press, Marine Science, Vol. 13, 239-256.

Austin, R.W. and T.J. Petzold, 1984: Spectral Dependence of the Diffuse Attenuation Coefficient of Light in Ocean Waters. *Proceedings SPIE*, Vol. 489, Ocean Optics VII, 168-178.

Baker, K.S. and R.C. Smith, 1979: Quasi-inherent characteristics of the Diffuse Attenuation Coefficient for Irradiance. *Proceedings SPIE*, Vol. 208, Ocean Optics VI, 60-63.

Baker, K.S. and R.C. Smith, 1982: Bio-optical Classification and Model of Natural Waters 2. *Limnology and Oceanography*, 27, 500-509.

Bartz, R., J.R.V. Zaneveld and H. Pak, 1978: A Transmissometer for Profiling and Moored Observations in Water. *Proceedings SPIE*, Vol. 160, Ocean Optics V, 107-108.

Bidigare, R.R., R.C. Smith, K.S. Baker and J. Marra, 1987: Oceanic Primary Production Estimates from Measurements of Spectral Irradiance and Pigment Concentrations. *Global Biogeochemical Cycles*, 1, 171-186.

Bidigare, R.R., J. Morrow and D.A. Kiefer, 1988: Derivative Analysis of Spectral Absorption by Phytoplankton Pigments. *Proceedings SPIE*, Vol. 925, Ocean Optics IX,

101-108.

Bidigare, R. R., J. H. Morrow and D.A. Kiefer, 1989: Spectral Absorption by Photosynthetic Pigments in the Northwestern Atlantic Ocean. *Journal of Marine Research*, in press.

Blasco, D., "1983". Packard and P.C. Garfield, 1982: Size Dependence of Growth Rate, Respiratory Electron Transport System Activity and Chemical Composition in Marine Diatoms in the Laboratory. *Journal of Phycology*, 18, 58-63.

Born, M. and E. Wolf, 1965: *Principles of Optics*, Pergamon Press, New York, 808p.

Bricaud, A., A. Morel and L. Prieur, 1983: Optical Efficiency Factors of Some Phytoplankters. *Limnology and Oceanography*, 28, 816-832.

Chamberlin, W. S., 1989: Light Absorption, Natural Fluorescence and Photosynthesis in the Open Ocean. Ph.D. Dissertation, University of Southern California, Los Angeles, California.

Collins, D. J., D.A. Kiefer, J.B. Soolhoo and I.S. McDermid, 1985: The Role of Reabsorption in the Spectral Distribution of Phytoplankton Fluorescence Emission. *Deep-Sea Research*, 32, 983-1003.

Collins, D. J., D.A. Kiefer, J.B. Soolhoo and C. Stallings, 1988a: The Remote Sensing of Oceanic Primary Productivity. in *Remote Sensing of Atmosphere and Oceans: Proceedings of the joint conference of the 4th Symposium of the international Society*

of Acoustic Remote Sensing and the 2nd Australasian Conference on the Physics of Remote Sensing of Atmosphere and Ocean. 52(1-6), Canberra, Australia, 16-24 February, 1988,

Collins, D.J., C.R. Booth, C.O. Davis, D.A. Kiefer and C. Stallings, 1988b: A Model of the Photosynthetically Available and Usable Irradiance in the Sea. Proceedings SPIE, Vol. 925, Ocean Optics IX, 87-100.

Davies-Colley, R. J., R.D. Pridmore and J.E. Hewitt, 1986: Optical Properties of Some Freshwater Phytoplanktonic Algae. *Hydrobiologia*, 133, 156-178,

Dugdale, R.C. and J.J. Goering, 1967: Uptake of New and Regenerated Forms of Nitrogen in Primary Productivity. *Limnology and Oceanography*, 12, 196-206.

Duntley, S. Q., 1963: Light in the Sea. *J. Optical Society of America*, 53, 214-233.

Faust, M.A. and K.H. Norris, 1982: Rapid *in vivo* Spectrophotometric Analysis of Chlorophyll Pigments in intact Phytoplankton Cultures. *British Phycological Journal*, 17, 351-?) 61.

Iturriaga, R., B.G. Mitchell and D.A. Kiefer, 1988: Microphotometric Analysis of Individual Particle, Absorption Spectra. *Limnology and oceanography*, 33, 128-135.

Jerlov, N.G. and E.S. Nielsen, 1974: *Optical Aspects of Oceanography*, Academic Press, New York, 494p.

Jerlov, N. G., ed., 1976: Marine Optics, Elsevier oceanography Series, 14, New York, 231 p.

Kiefer, D.A. and R.W. Austin, 1974: The Effect of Varying Phytoplankton Concentration on Submarine light Transmission in the Gulf of California. Limnology and Oceanography, 19, 55-64.

Kiefer, D.A. and J. I]. Soohoo, 1982: Spectral Absorption by Marine Particles of Coastal Waters of Baja California. Limnology and Oceanography, 27, 492-499,

Kiefer, D.A. and B.G. Mitchell, 1983: A Simple, Steady State Description of Phytoplankton Growth Based on Absorption Cross Section and Quantum Efficiency. Limnology and Oceanography, 28, 770-776.

Kiefer, D. A., 1984: Microplankton and Optical Variability in the Sea: Fundamental Relationships. Proceedings SPIE, Vol. 489, Ocean Optics VII, 42-48.

Kiefer, D. A., C.R. Booth and W.S. Chamberlain, 1989: Natural Fluorescence. Limnology and oceanography, in press.

Kirk, J. T. O., 1986: Light and Photosynthesis\_ in Aquatic Ecosystems. Cambridge [University Press, N. Y., 401p.

Kishino, M., S. Sugihara, and N. Okami, 1984: Estimation of Quantum Yield of Chlorophyll a Fluorescence from the Upward Irradiance Spectrum in the Sea. La Mer, 22, 233-240.

Laws, E.A. and T.T. Bannister, 1980: Nutrient- and Light-Limited Growth of *Thalassiosira fluviatilis* in Continuous Culture, with Implications for Phytoplankton Growth in the Ocean. *Limnology and Oceanography*, 25, 457-473.

Lieberman, S.H., G.D. Gilbert, P.F. Seligman and A.W. Dibelka, 1984: Relationship Between Chlorophyll *a* Fluorescence and Underwater Light Transmission in Coastal Waters off Southern California. *Deep-Sea Research*, 31, 171-180.

Morel, A. and I. Prieur, 1977: Analysis of Variations in Ocean Color. *Limnology and Oceanography*, 22, 709-722.

Morel, A., 1978: Available, Usable, and Stored Radiant Energy in Relation to Marine Photosynthesis. *Deep-Sea Research*, 25, 673-688.

Morel, A. and A. Bricaud, 1981: Theoretical Results Concerning Light Absorption in a Discrete Medium, and Application to Specific Absorption of Phytoplankton. *Deep-Sea Research*, 28, 1375-1393.

Morel, A. and R.C. Smith, 1982: Terminology and Units in Optical oceanography. *Marine Geodesy*, 5, 335-349.

Morel, A., 1987: Chlorophyll-Specific Scattering Coefficient of Phytoplankton. A Simplified Theoretical Approach. *Deep-Sea Research*, 34, 1093-1105.

Morel, A., 1988: Optical Modeling of the Upper Ocean in Relation to its Biogenous

Matter Content (Case 1 Waters). J. Geophysical Research, 93, (C9), 10749-10768.

Morrow, J.H., 1988: Light Absorption in Naturally occurring Marine Phytoplankton Communities. Ph.D. Dissertation, University of Southern California, Los Angeles, California, 138P.

Morrow, J.H., W.S. Chamberlin and D.A. Kiefer, 1989: A Two Component Description of Spectral Absorption by Marine Particles. submitted to Limnology and Oceanography.

Pak, H., D.A. Kiefer and J.C. Kitchen, 1988: Meridional Variations in the Concentration of Chlorophyll and Microparticles in the North Pacific Ocean. Deep-Sea Research, 35, 1151-1171.

Peterson, D.H., M.J. Perry, K.F. Bencala and M.C. Talbot, 1987: Phytoplankton Productivity in Relation to Light Intensity: A Simple Equation. J. Estuarine, Coastal and Shelf Science., 24, .

Platt, "T.", 1986: Primary Production of the Ocean Water Column as a Function of Surface Light intensity: Algorithms for Remote Sensing, Deep-Sea Research, 33, 149-163,

Platt T. and S. Sathyendranath, 1988: Oceanic Primary Production: Estimation by Remote Sensing at Local and Regional Scales. Science, 41, 1613-1620.

Preisendorfer, R. W., 1976: Hydrologic Optics, Volumes I-IV, U.S. Department of Commerce, National Oceanic and Atmospheric Administration, Environmental Research Laboratories.

Prieur, L. and S. Sathyendranath, 1981: An Optical Classification of Coastal and Oceanic Waters Based on the Specific Spectral Absorption Curves of Phytoplankton Pigments, Dissolved Organic Matter, and Other Particulate Materials. *Limnology and Oceanography*, 26, 671-689.

Ryther, J.H. and C.S. Yentsch, 1957: The Estimation of Phytoplankton Production in the Ocean from Chlorophyll and Light Data. *Limnology and Oceanography*, 2, 281-286.

Siegel, D.A. and W.H. Dickey, 1987a: Observations of the Vertical Structure of the Diffuse Attenuation Coefficient Spectrum. *Deep-Sea Research*, 34, 547-563.

Siegel, D.A. and W.H. Dickey, 1987b: On the Parameterization of Irradiance for Open Ocean Photoprocesses. *J. Geophysical Research*, 92, (C13), 14648-14662.

Smith, R.C. and K.S. Baker, 1978a: The Bio-optical State of Ocean Waters and Remote Sensing. *Limnology and Oceanography*, 23, 247-259.

Smith, R.C. and K.S. Baker, 1978b: Optical Classification of Natural Waters. *Limnology and Oceanography*, 23, 260-267.

Sollito, J.B., D.A. Kiefer, D.J. Collins and L.S. McDermid, 1986: In vivo Fluorescence Excitation and Absorption Spectra of Marine Phytoplankton: I. Taxonomic Characteristics and Response to Photoadaptation. *J. Plankton Research*, 8, 197-214.

Sverdrup H.U., 1953: On Conditions for Vernal Blooming of Phytoplankton. *J. Cons.*

Perm. Int. Explor. Mer, 18, 287-? 95.

Topliss, B.J. and T. Platt, 1986: Passive Fluorescence and Photosynthesis in the Ocean: implications for Remote Sensing, *Deep-Sea Research*, 33, 849-864,

van de Hulst, H.C., 1983: Multiple Light Scattering: Tables, Formulas and Applications, volumes 1, 11. Academic Press, N. Y., 739p.

Yentsch, C. S., 1962: Measurement of Visible Light Absorption by Particulate Matter in the Ocean. *Limnology and Oceanography*, 7, 207-217.

Zaneveld, J.R.V. and H.J. Pak, 1979: Optical and Particulate Properties at Oceanic Fronts, *J. Geophysical Research*, 84, (C12), 7781-7790.

## Figure Captions

### Figure 2-1:

Conceptual transformation of Carbon and Nitrogen within the phytoplankton community.

### Figure 2-2:

The partitioning of energy by the phytoplankton cell through absorption and scattering. The absorbed radiant energy is further partitioned into heat, fluorescence and the assimilation of Carbon, Nitrogen and other compounds through photosynthetic processes.

### Figure 2-3:

The propagation of light energy in the ocean, illustrating the effects of absorption and scattering on the geometry of the light field at depth, and the relationship between the upwelling radiance,  $I_u(\lambda)$ , and the water-leaving radiance,  $I_w(\lambda)$ .

### Figure 2-4:

The spectral distribution of the attenuation coefficient,  $a(\lambda)$ , as the sum of the water,  $a_w(\lambda)$ , phytoplankton,  $a_p(\lambda)$ , and detrital,  $a_d(\lambda)$ , components. The water component,  $a_w(\lambda)$ , and the water scattering coefficient,  $b_w(\lambda)$ , are derived from Morel and Prieur (1977). The phytoplankton component is derived from the results of the work of Soolhoo, et al. (1986) and of Collins, et al. (1988b) assuming a pigment concentration of  $5.0 \mu\text{g/l}$ . The detrital component is derived from Morel and Prieur (1977), corresponding to a scattering coefficient of  $2.0 \text{ m}^{-1}$  at 550 nm,

Figure 2-5:

The vertical distribution of the mean value of the spectral absorption coefficient,  $a_p(\lambda, z)$ , for data collected on Biowatt 11 during August, 1987 in the southern Sargasso Sea. Data from Chamberlin (1989), demonstrating a deep particle maximum.

Figure 2-6:

The spectral distribution of the chlorophyll *a* specific particulate absorption coefficient,  $a_p^*(\lambda, z)$ , as a function of depth. Data from the BLOWATT 11 cruise in the Sargasso Sea, August, 1987. The data from Chamberlain (1989) indicates the variability of the contribution from the detrital material to the total spectrum and the increased pigment concentration per cell at low light levels.

Figure 2-7:

The *in vivo* absorption spectrum for particulate material obtained from the Sargasso Sea at a depth of 107 m from the BLOWATT I cruise, 1985. a: The particulate absorption spectrum with the location of significant pigments contributing to the spectrum indicated. b: The fourth derivative of the spectrum, illustrating the pigment composition of the sample. The analysis uses the techniques of Bidigare, Morrow and Kiefer (1988a). Data from Morrow (1988).

Figure 2-8:

An illustration of the decomposition of the spectrum for particulate absorption into phytoplankton and detrital components. a: The total particulate absorption coefficient,  $a_p(\lambda)$ , together with the phytoplankton,  $a_p(\lambda)$ , and detrital,  $a_d(\lambda)$ ,

components which contribute to the spectrum. The upper dashed line is the reconstructed spectrum. b: The regression of the particulate absorption coefficient,  $a_p(440)$ , against the chlorophyll *a* concentration. The open circles represent the total  $a_p(440)$ , while the dark triangles represent the phytoplankton component. Data from Morrow (1988).

Figure 2-9:

The efficiency factors for absorption,  $Q_a(\rho)$ , and for attenuation,  $Q_{atten}(\rho)$ , as a function of a wavelength dependent parameter,  $\rho$ . The functional form for  $Q_a(\rho)$  is derived from van de Hulst (1983) and is illustrated in Collins, et al. (1986). In this case,  $\rho$  is the optical density of the central ray propagating through the particle. The functional form for  $Q_{atten}(\rho)$ , the efficiency factor for scattering in the case of non-absorbing spheres, is given by van de Hulst (1983) and by Kirk (1986). In this case,  $\rho$  is the phase lag for light propagating along the central ray of the particle.

Figure 2-10:

The cellular pigment concentration in both laboratory cultures and field samples as a function of cell diameter, illustrating the packaging of cellular material for cells of a wide range of sizes. Data from Blasco et al. (1982), Davies-Colley et al. (1986) and Morel (1987). Figure from Morrow (1988).

Figure 2-11:

The concentration of marine particles as a function of particle volume in near-surface water. Data from Zaneveld and Pak (1979) obtained at a number of stations at differing distances offshore. The increased concentration of large particles is representative of terrigenous material.

Figure 2-12:

The variation of suspended particle concentration as a function of beam attenuation coefficient,  $c(665)$ , for samples from the northeastern Pacific Ocean. Data from Pak, et al. (1988) indicate differing regressions in this relationship caused by the changes in particle size distribution with depth.

Figure 2-13:

The beam attenuation coefficient,  $c(660)$ , as a function of the pigment concentration for waters in the central North Pacific Ocean at the ODEX site. 1: Surface mixed layer for which the pigment concentration is vertically uniform. 2: The region between the bottom of the mixed layer and the particle maximum. 3: The region between the particle maximum and the chlorophyll  $a$  maximum. In this region, photoadaptive processes cause significant changes in the pigment concentration per cell. 4: The region below the chlorophyll  $a$  maximum. In this region, as a consequence of the low available irradiance, further changes in the pigment concentration per cell do not occur.

Figure 2-14:

The pigment specific beam attenuation coefficient as a function of the optical depth in terms of  $K_{par}$ . Data from the ODEX cruise, 1982, from Kiefer (1984). The uniform regions correspond to the surface mixed layer for each profile.

Figure 2-15:

The downwelling irradiance field in the ocean computed assuming a vertically uniform pigment field, from the work of Morel (1988) and of Collins, et al. (1988 b).

a: The vertical distribution of the downwelling  $E_{par}(z)$  as a function of pigment concentration. b: The vertical distribution of the downwelling spectral irradiance computed for a pigment concentration of  $5 \mu\text{g/l}$ .

Figure 2-16:

The average cosine of the downwelling irradiance and the scalar irradiance fields as a function of the optical depth, for a ratio of scattering to absorption,  $b/a = 5.0$ , from Kirk (1986) for vertically incident light at the sea surface,

Figure 2-17:

The spectral distribution of the diffuse attenuation coefficient,  $k(\lambda)$ , as the sum of the water,  $k_w(\lambda)$ , and phytoplankton,  $k_p(\lambda)$ , components. Computed from the theory of Morel (1988) and Collins, et al. (1988b) for a pigment concentration of  $5.0 \mu\text{g/l}$ . Data for  $k_w(\lambda)$  from Baker and Smith (1982).

Figure 2-18:

The dependence of the diffuse attenuation coefficient for downwelling irradiance,  $k_d(\lambda, \text{pigment})$ , on the pigment concentration. Computed from Morel (1988) and Collins, et al. (1988 b).

Figure 2-19:

The dependence of the diffuse attenuation coefficient for downwelling photosynthetically available irradiance,  $K_{par}(\text{pigment})$ , on the pigment concentration. Computed from the theory of Morel (1988) and Collins, et al. (1988b) for the 50%, 10% and 1%  $E_{par}$  levels.

Figure 2-20:

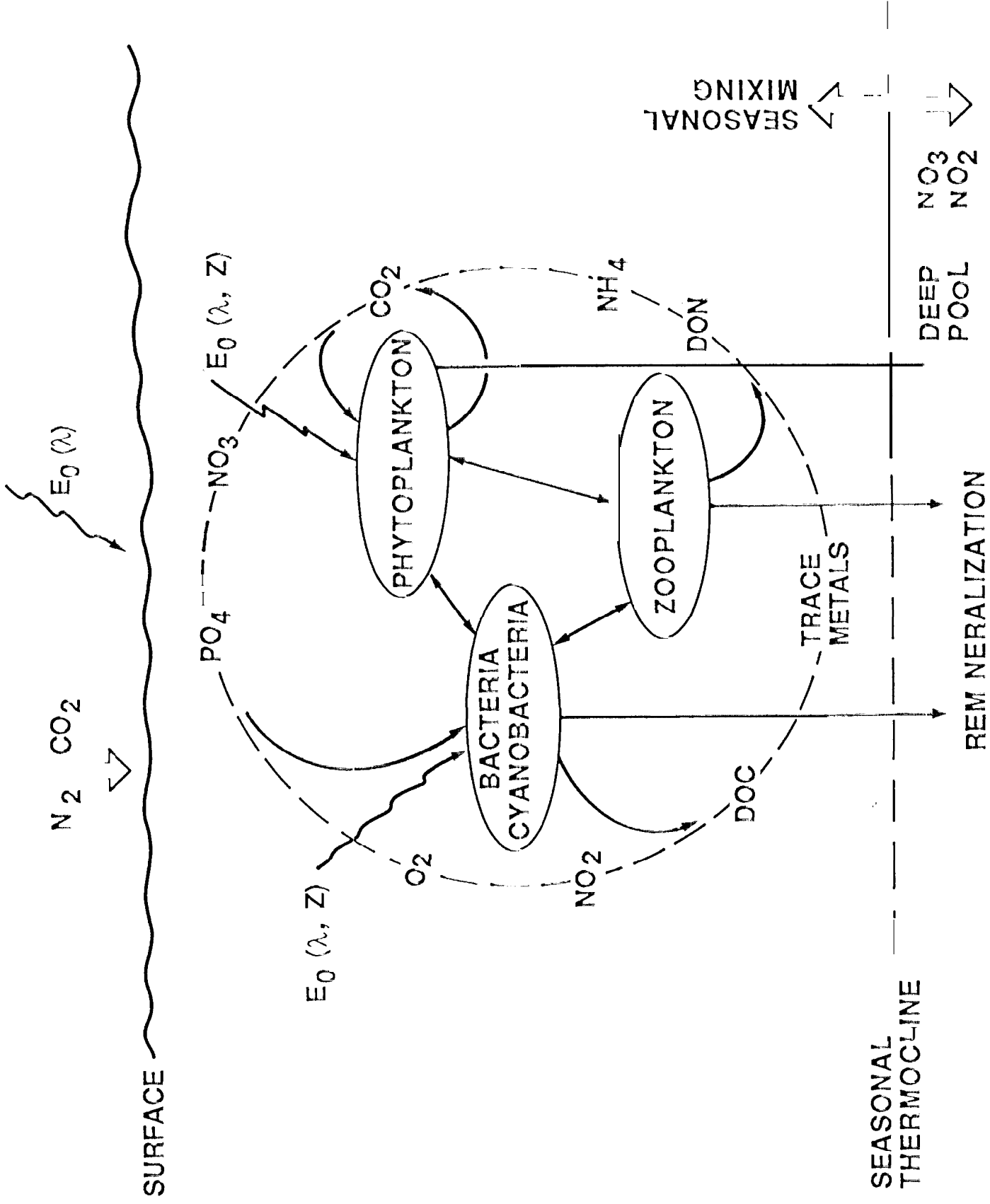
The relationship between the depth distributions of the absorbed radiant energy,  $E_{\text{pur}}$ , and the photosynthetically available irradiance,  $E_{\text{par}}$ , as a function of pigment concentration in the water column for vertically uniform pigment distributions. Computed from the theory of Collins, et al. (1988 b).

Figure 2-21:

The spectral distribution of the downwelling irradiance,  $E_d(\lambda, Z)$ , as a function of depth for two values of the pigment concentration. Computed from the theory of Collins, et al. (1988 b). This figure illustrates the spectral narrowing of the light field with increasing pigment concentration. a: Pure sea water. b: 5  $\mu\text{g/l}$  pigment concentration.

Figure 2-22:

The vertical distribution of the optical properties in the sea from Siegel and Dickey (1987a) for the ODEX, 1982 cruise. a: The vertical distribution of the mean potential density, beam attenuation,  $c(660)$ , chlorophyll *a* fluorescence, chlorophyll *a* and phaeopigments. b: The vertical distribution of the diffuse attenuation coefficient for downwelling irradiance at selected wavelengths. The dashed line in each panel is the value of  $k_w(\lambda)$ , the diffuse attenuation coefficient for pure water at that wavelength.



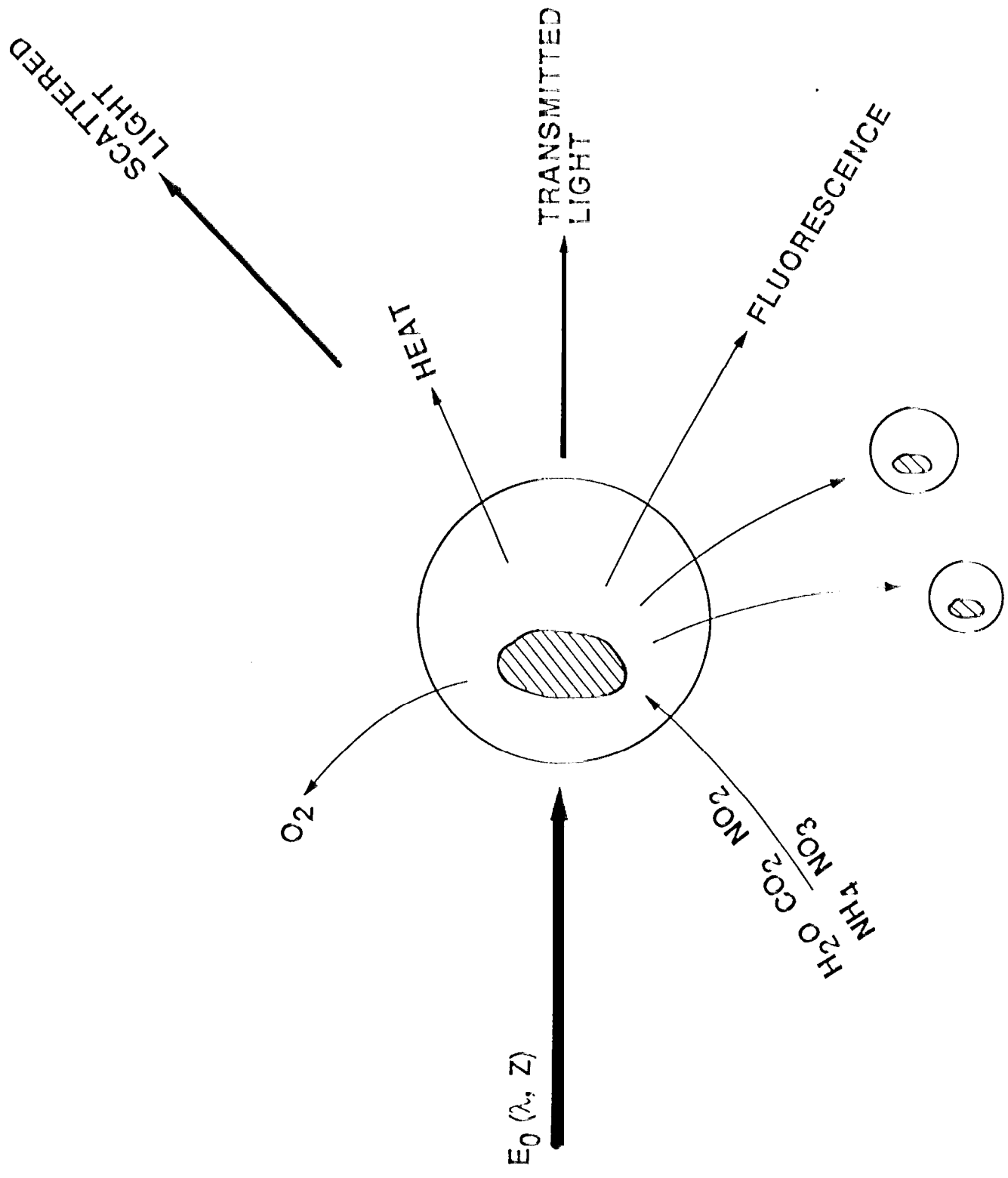


Figure 1

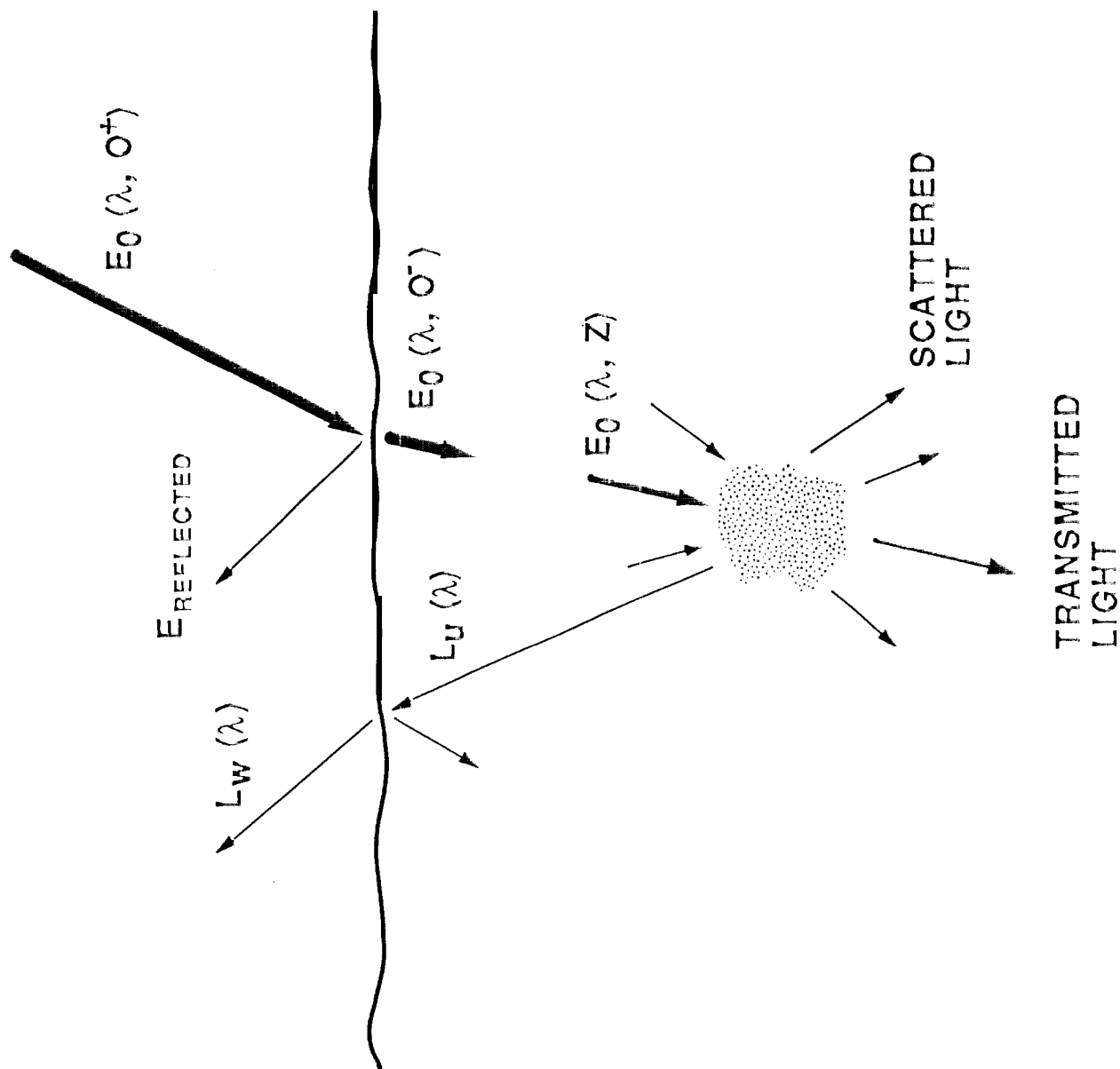
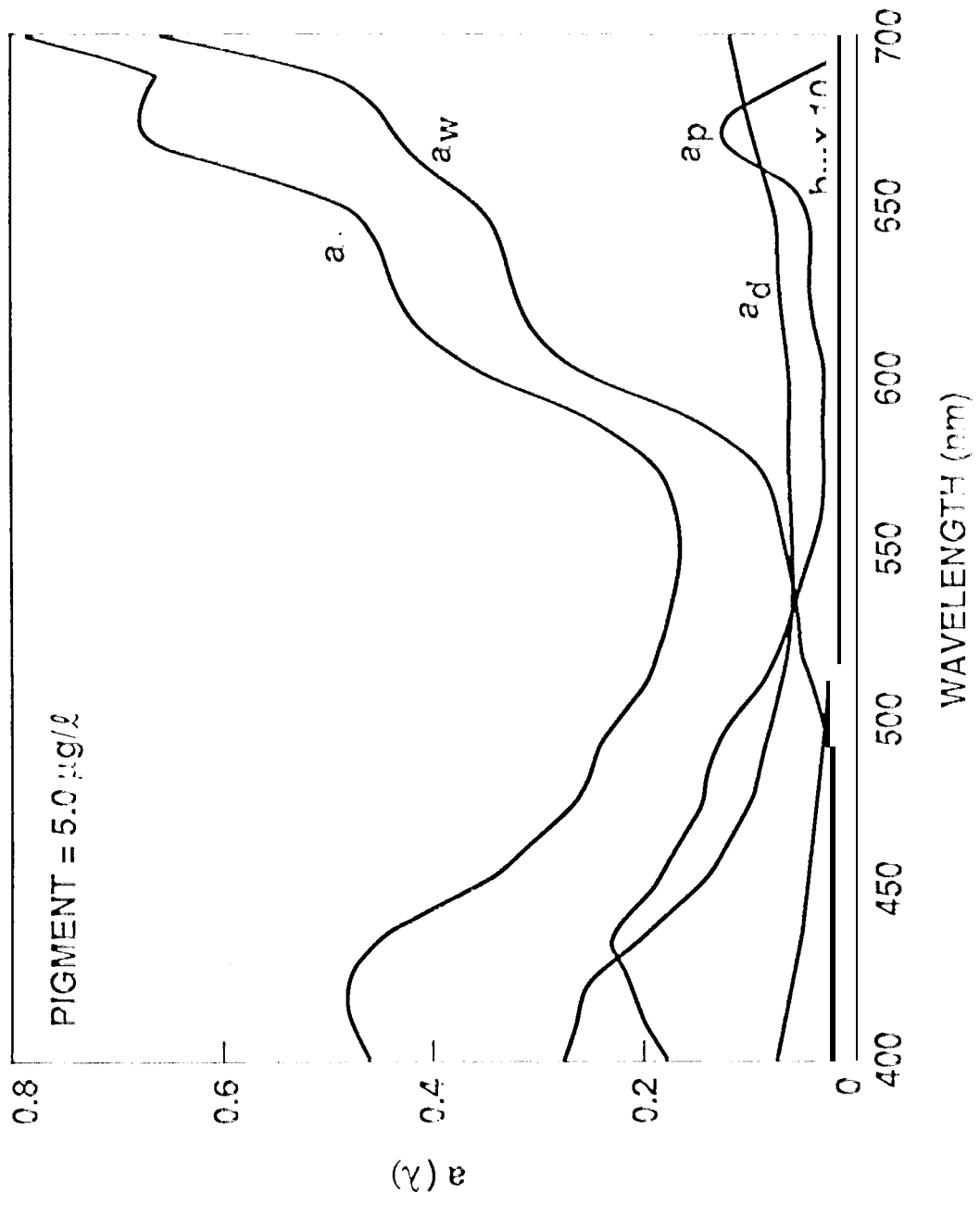


Figure 3



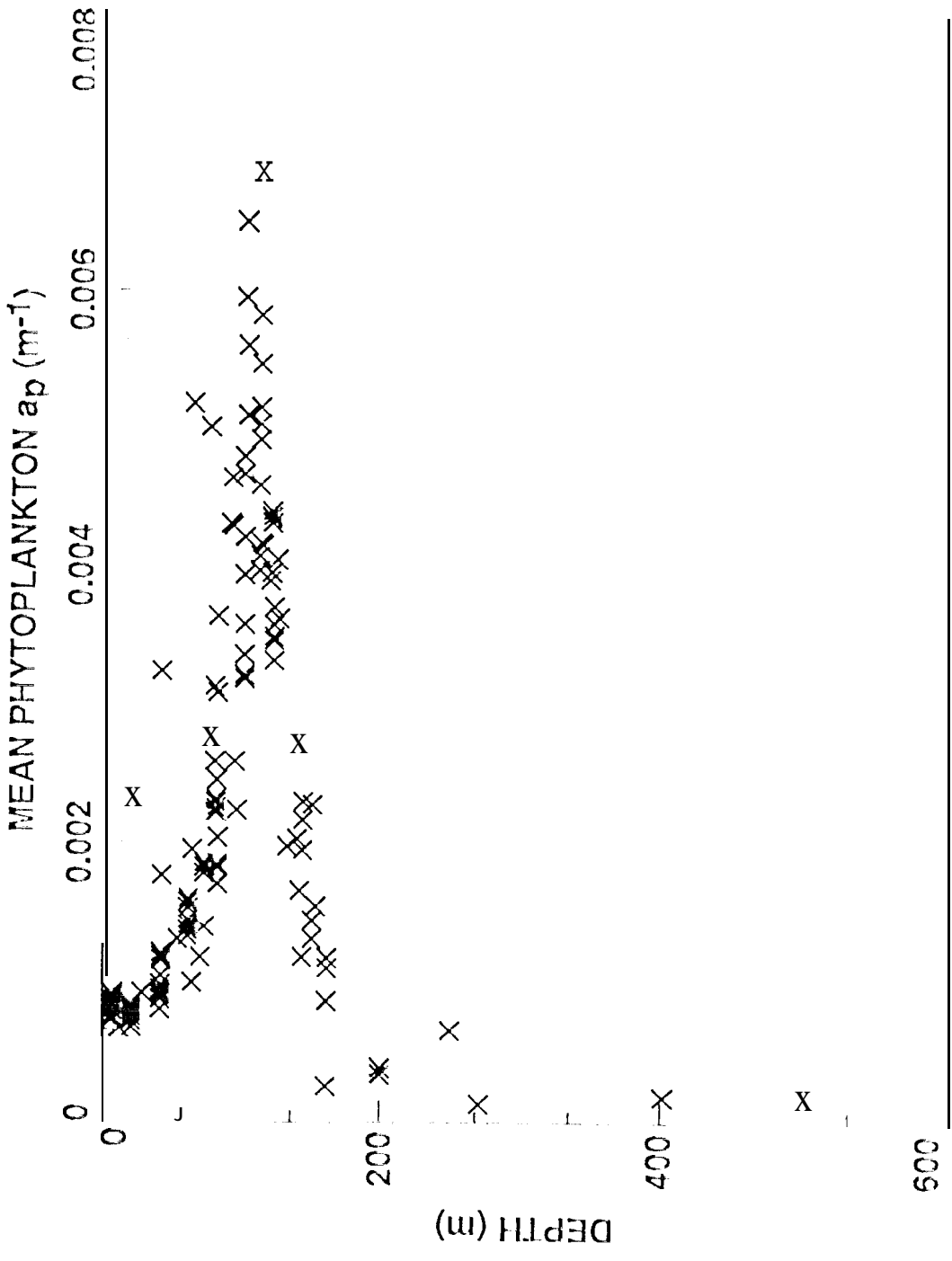


Figure 5

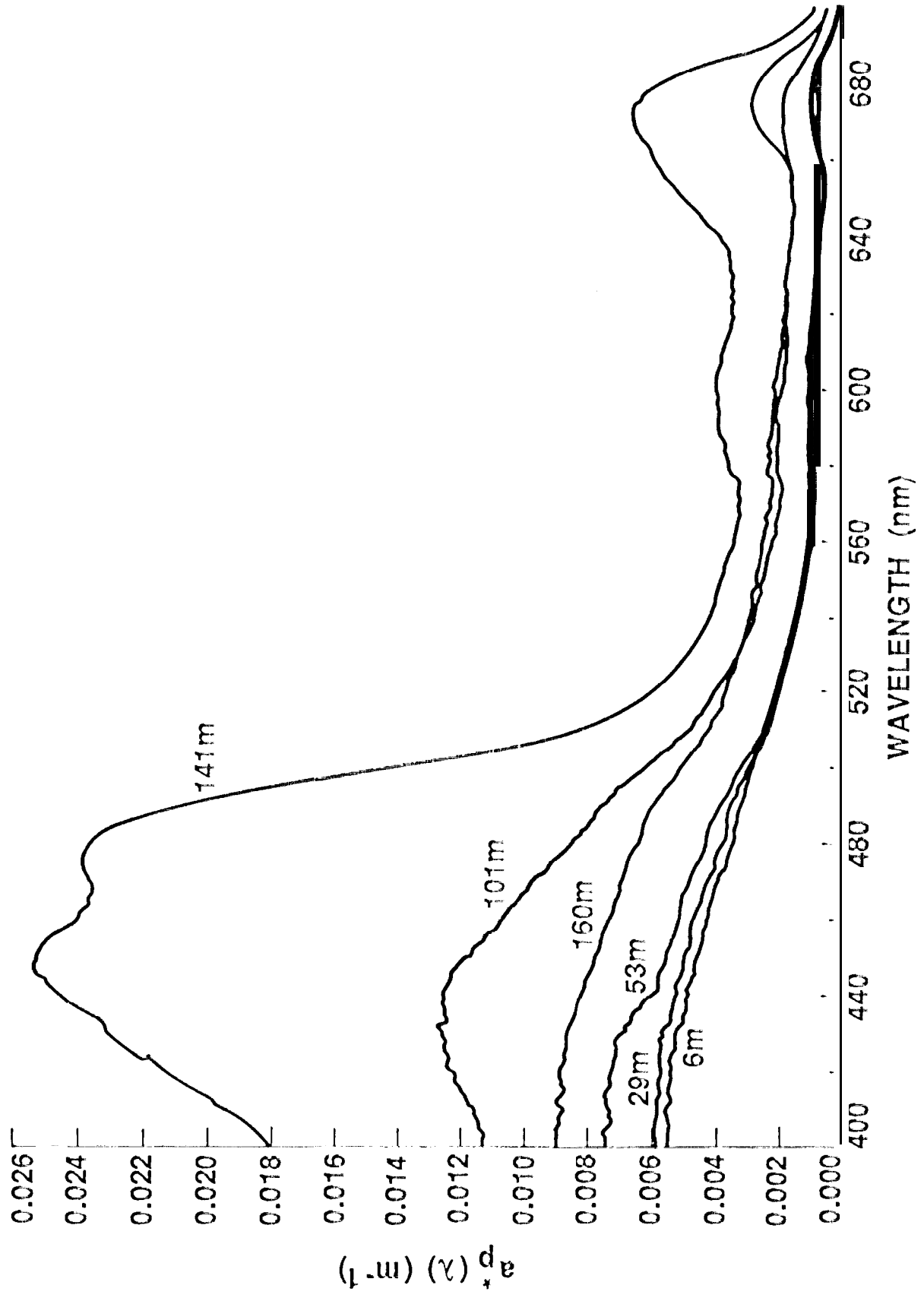


Figure 6

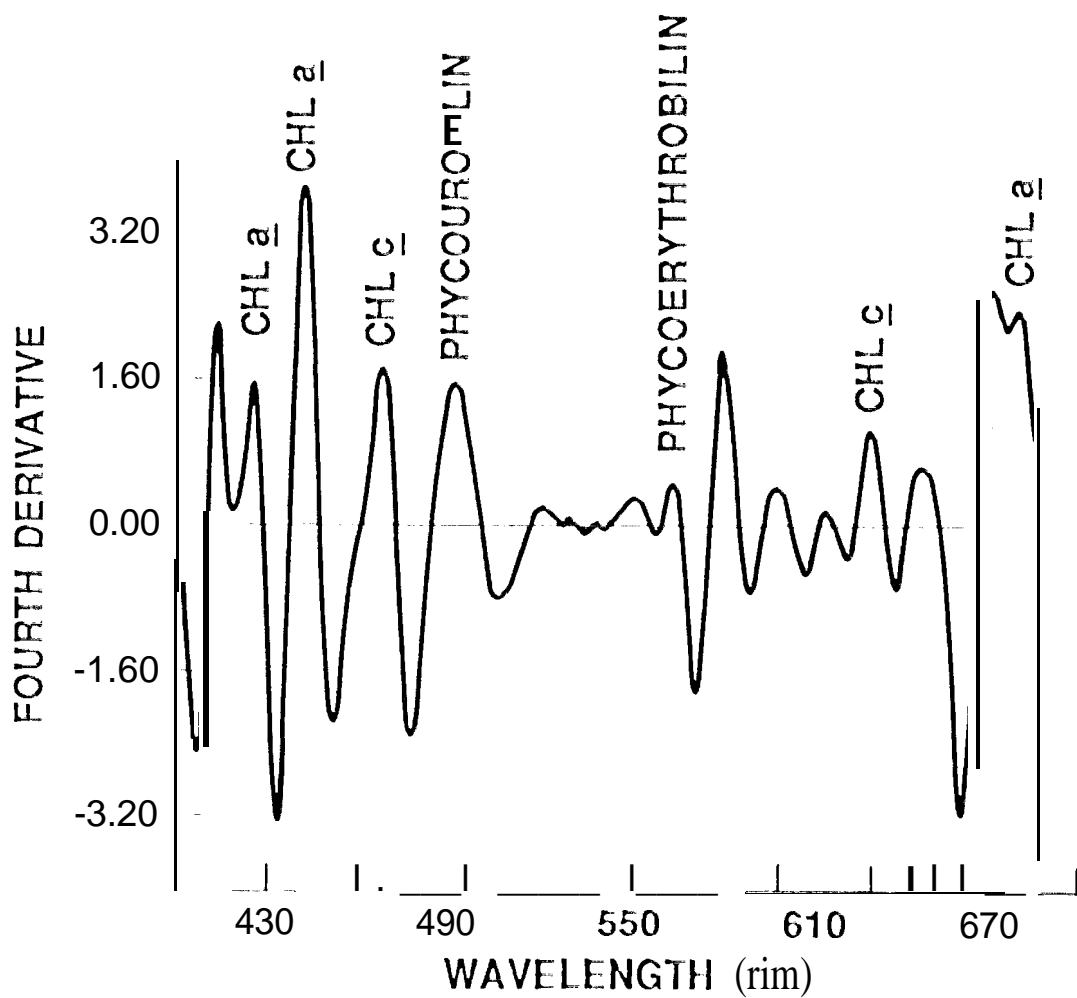
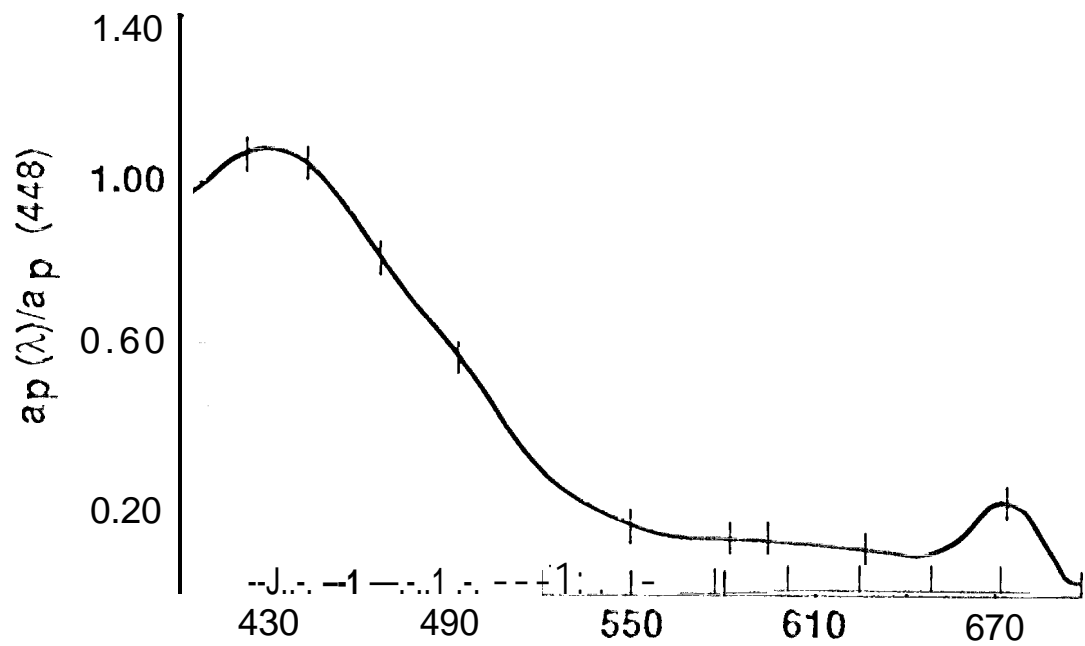
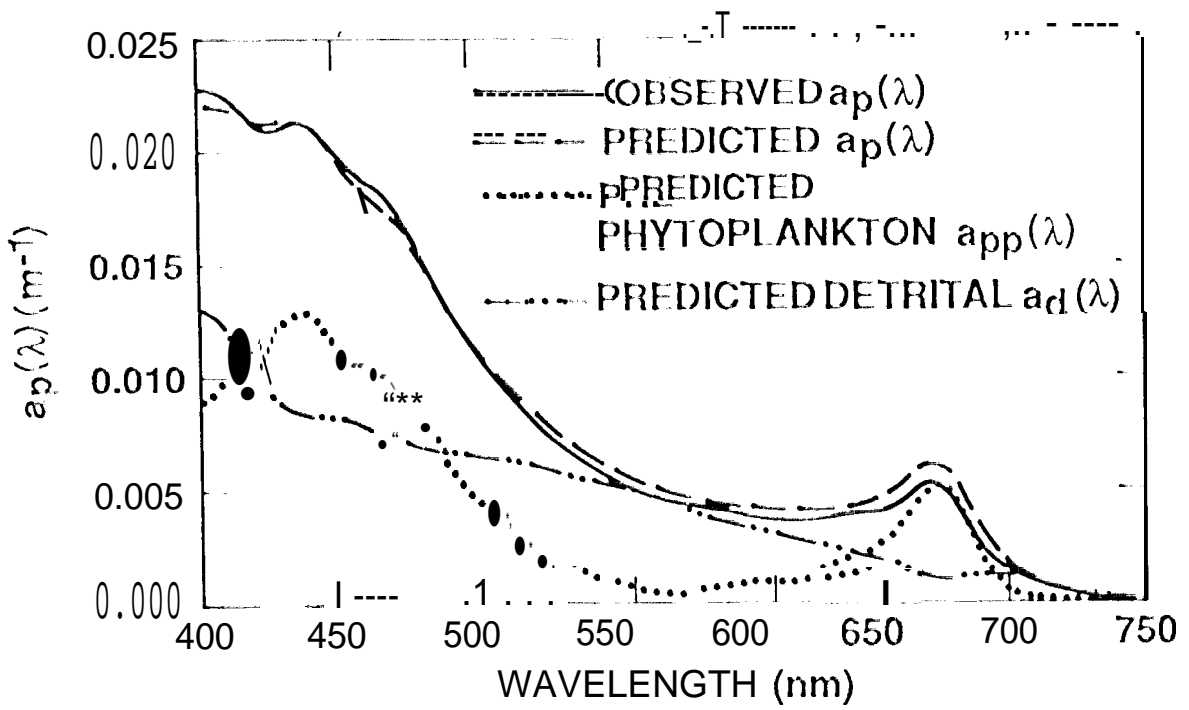
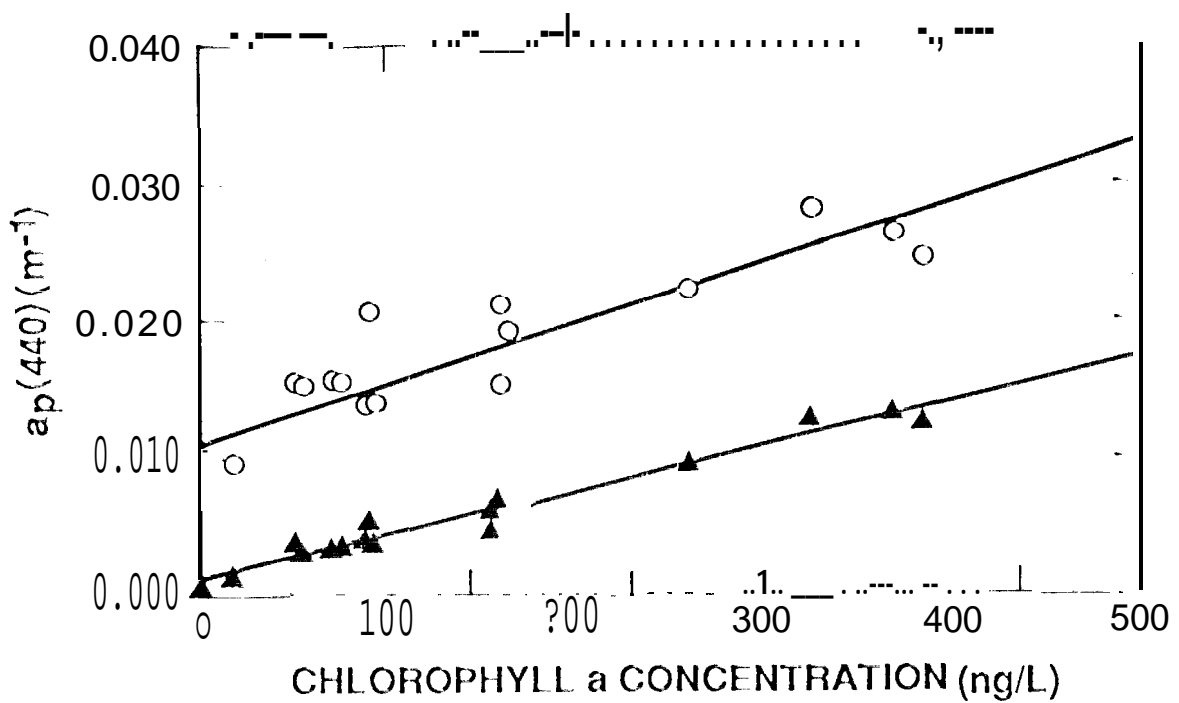


Figure 7



a. SPECTRAL DECOMPOSITION



b. CHLOROPHYLL a REGRESSION

Figure 8

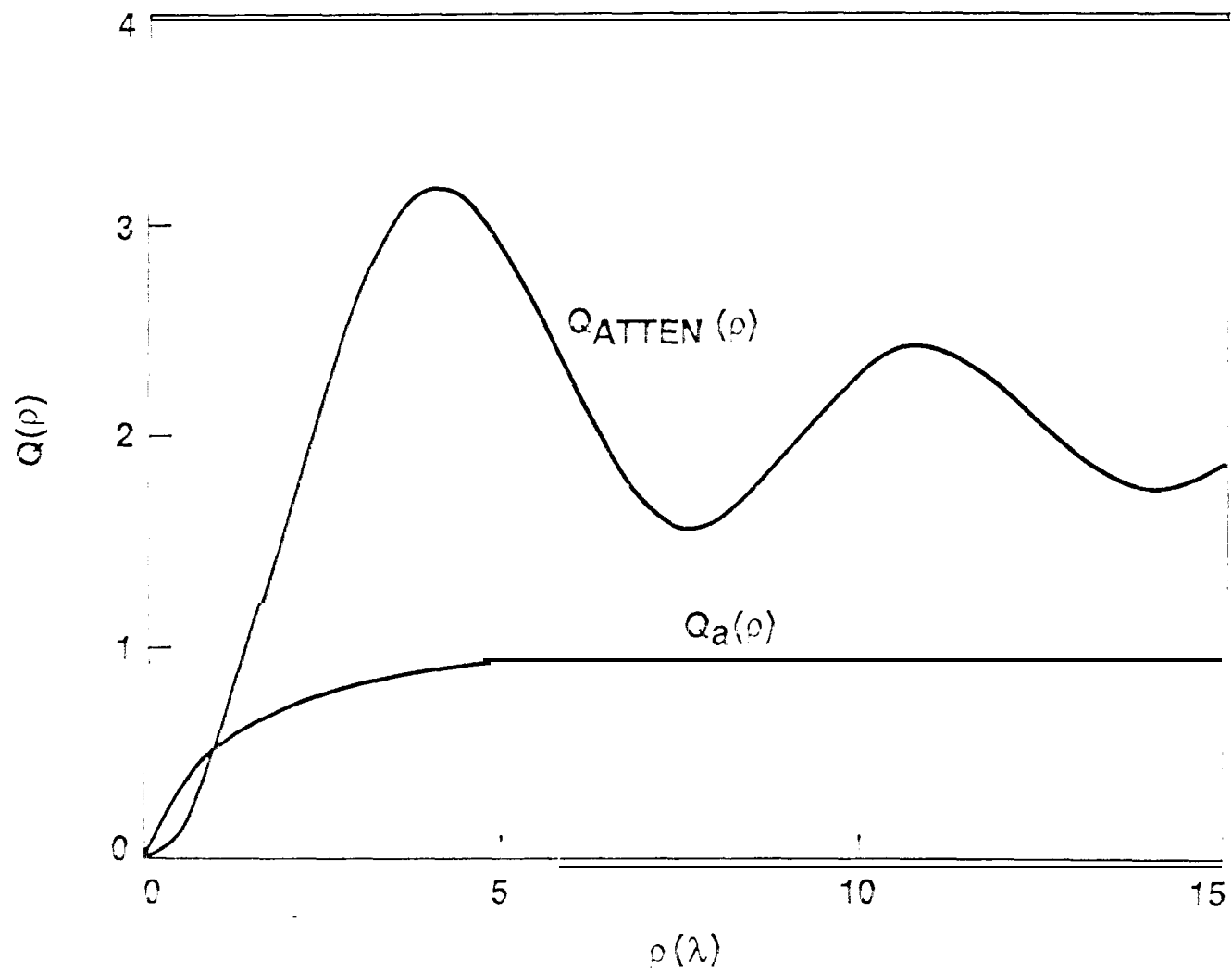


Figure 4

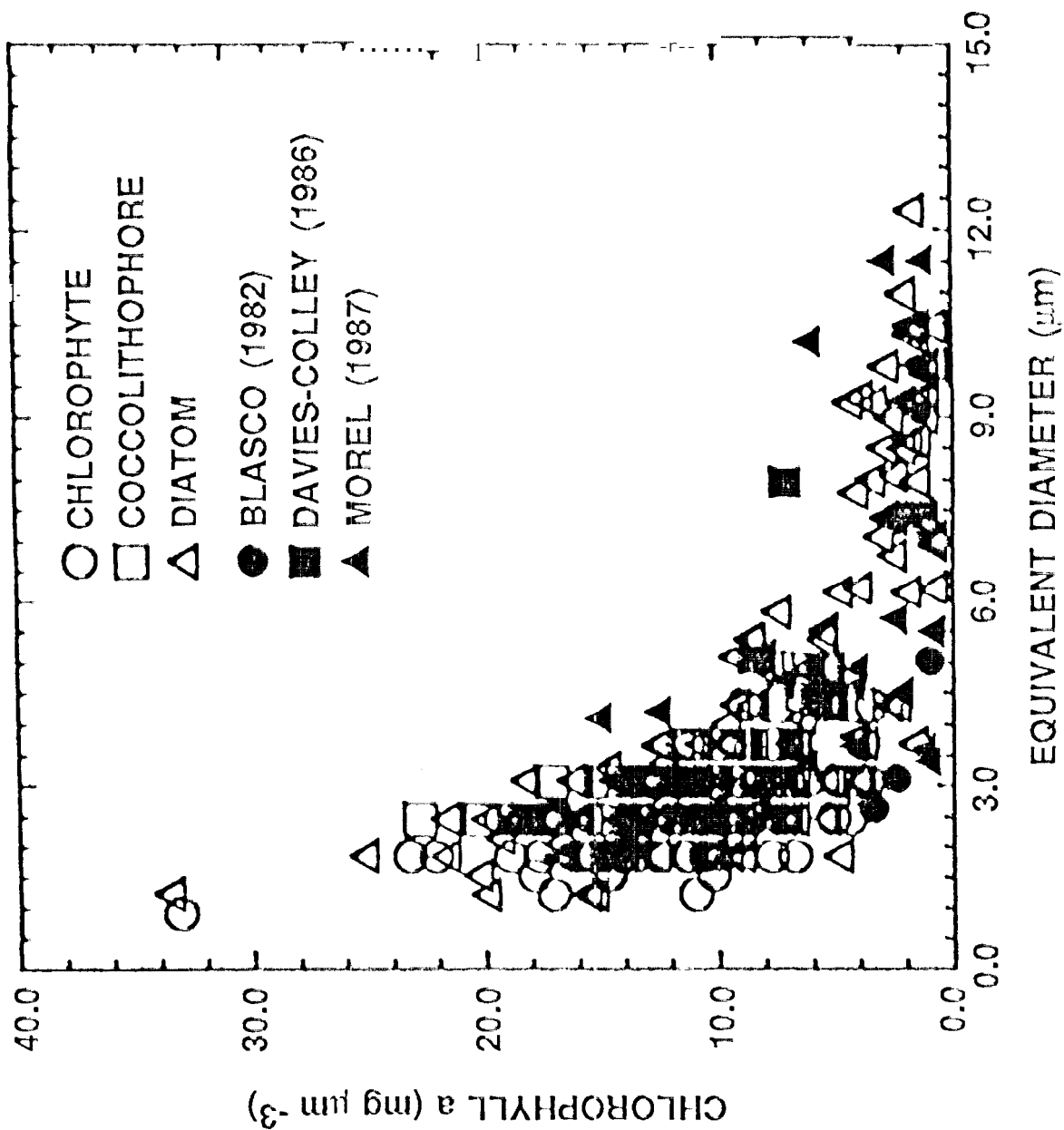


Figure 10

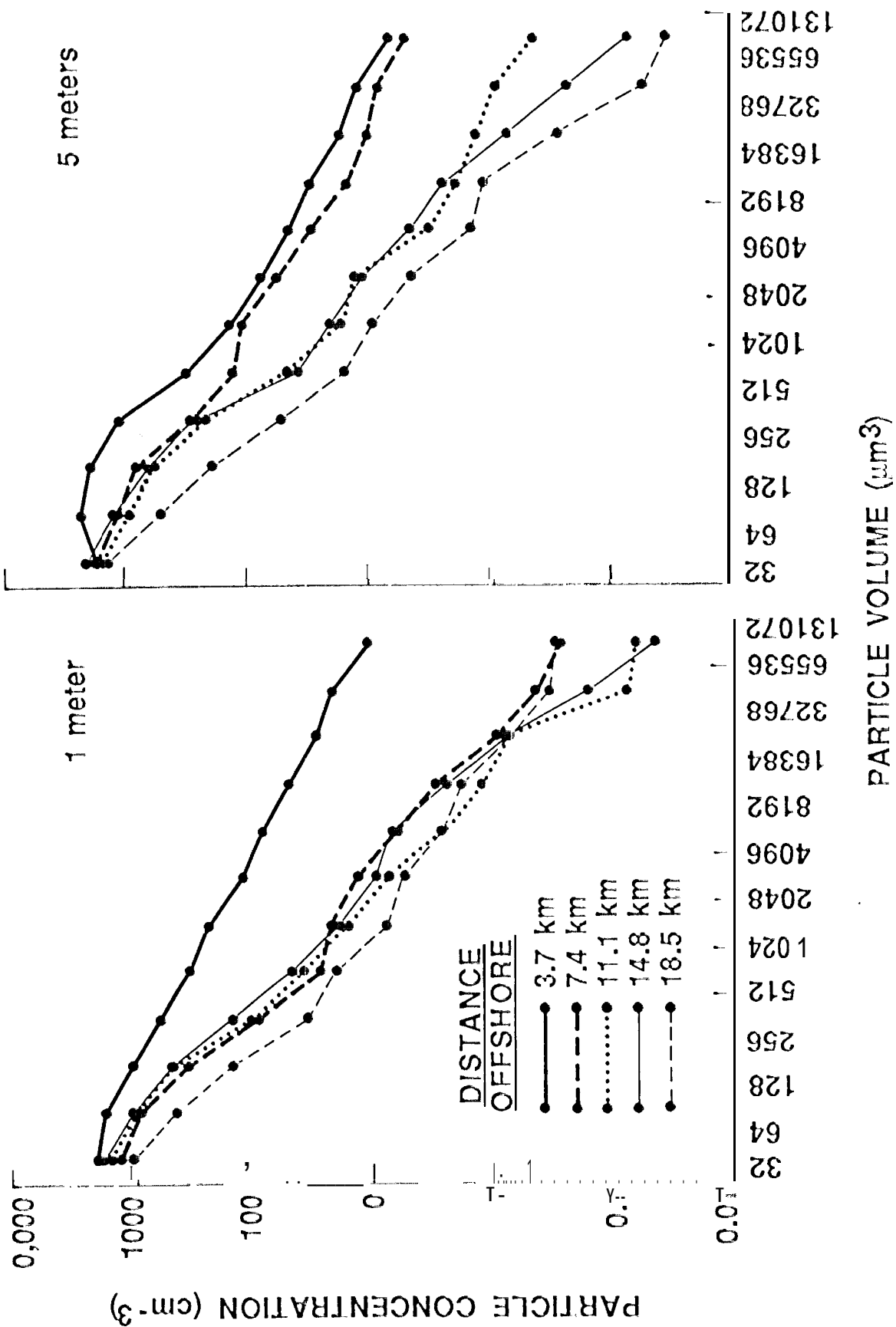


Figure 11

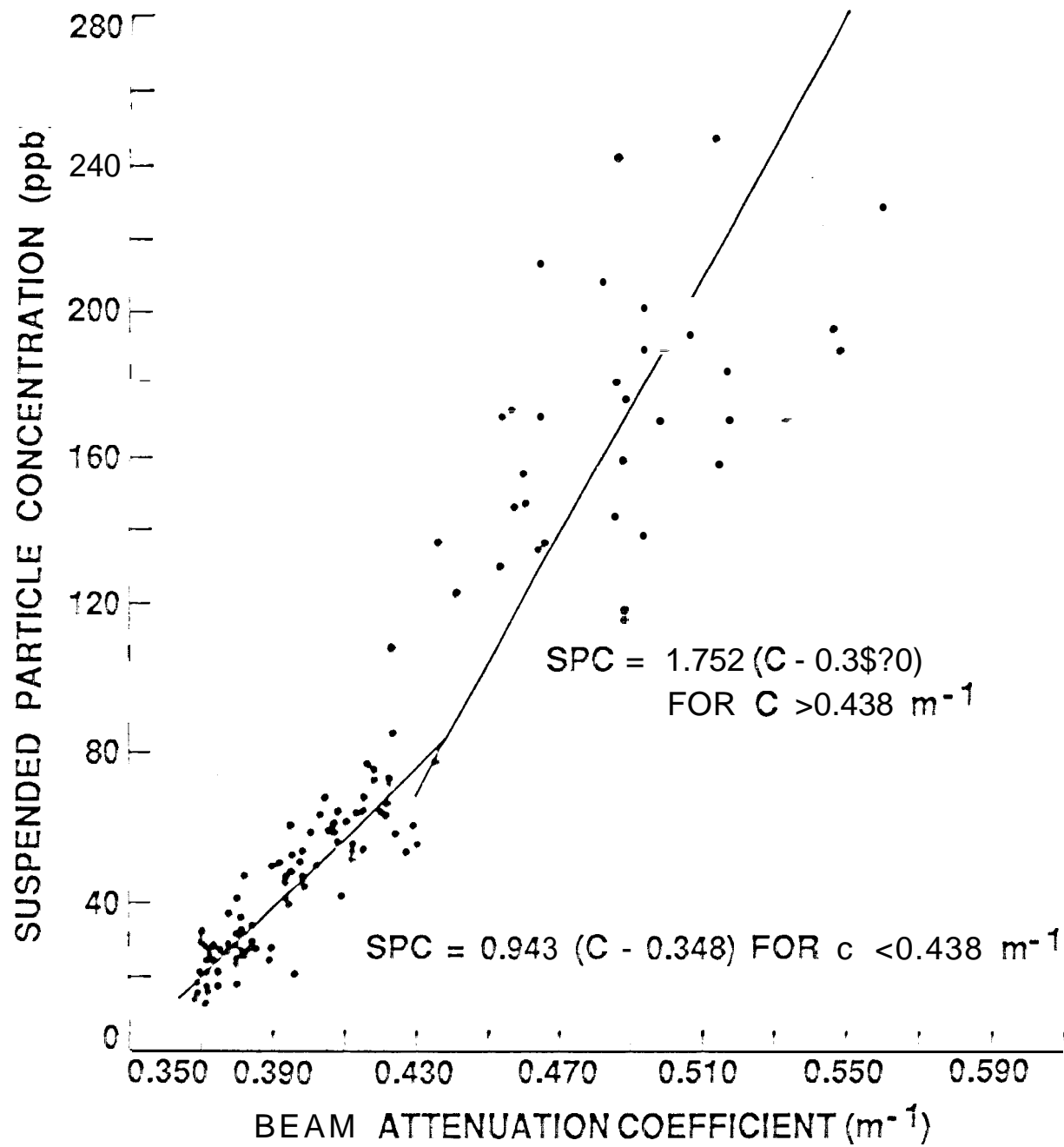


Figure 17

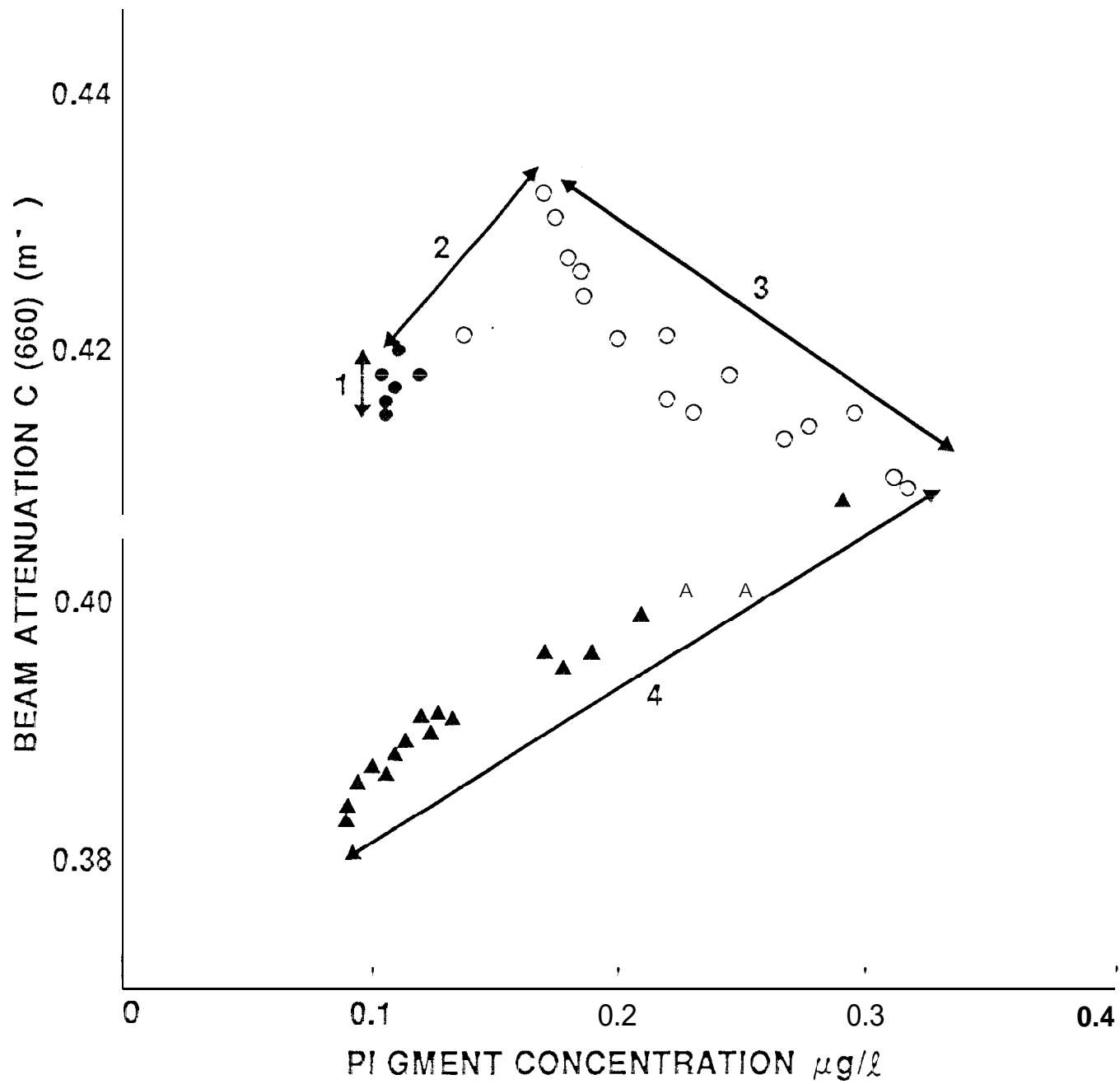
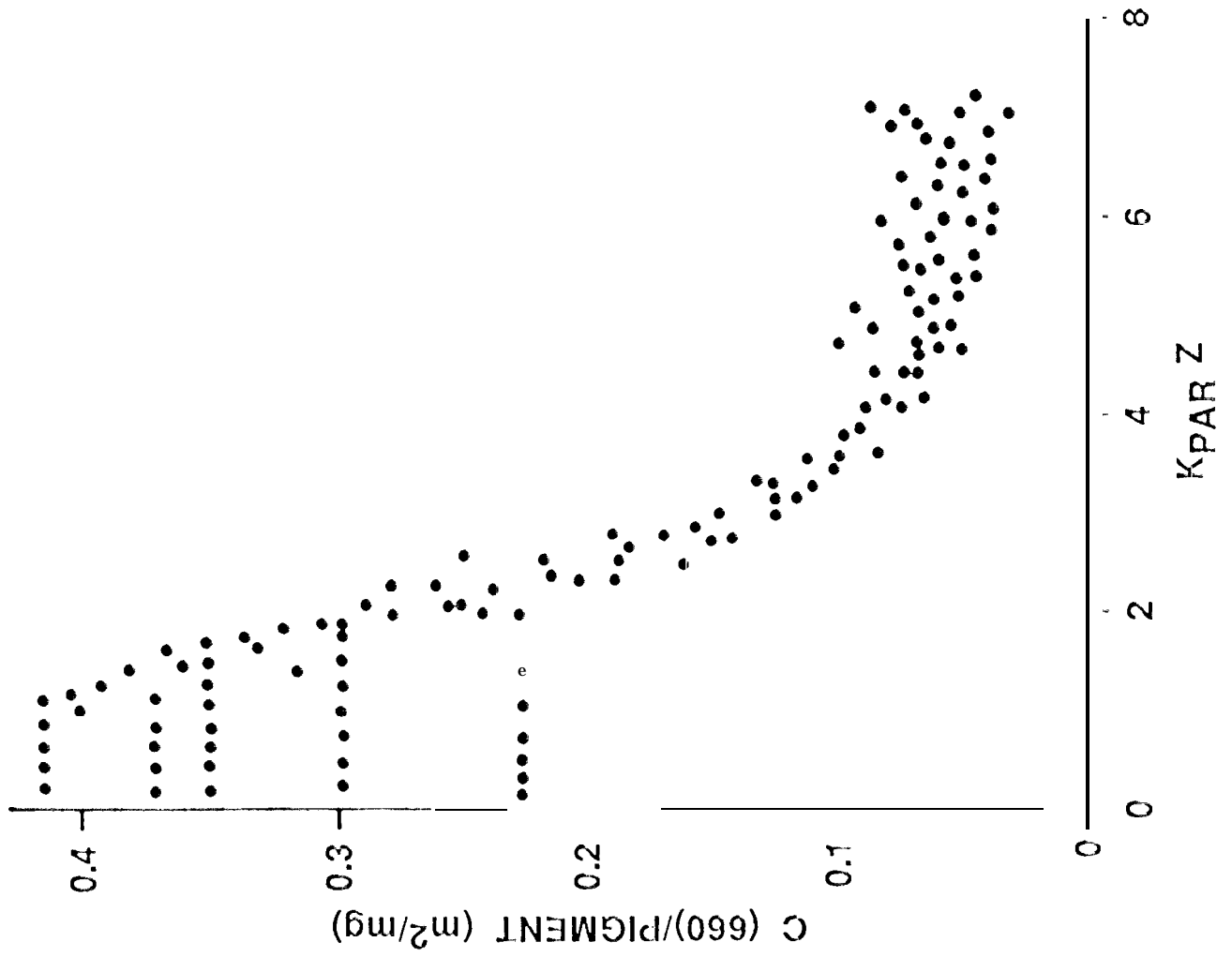
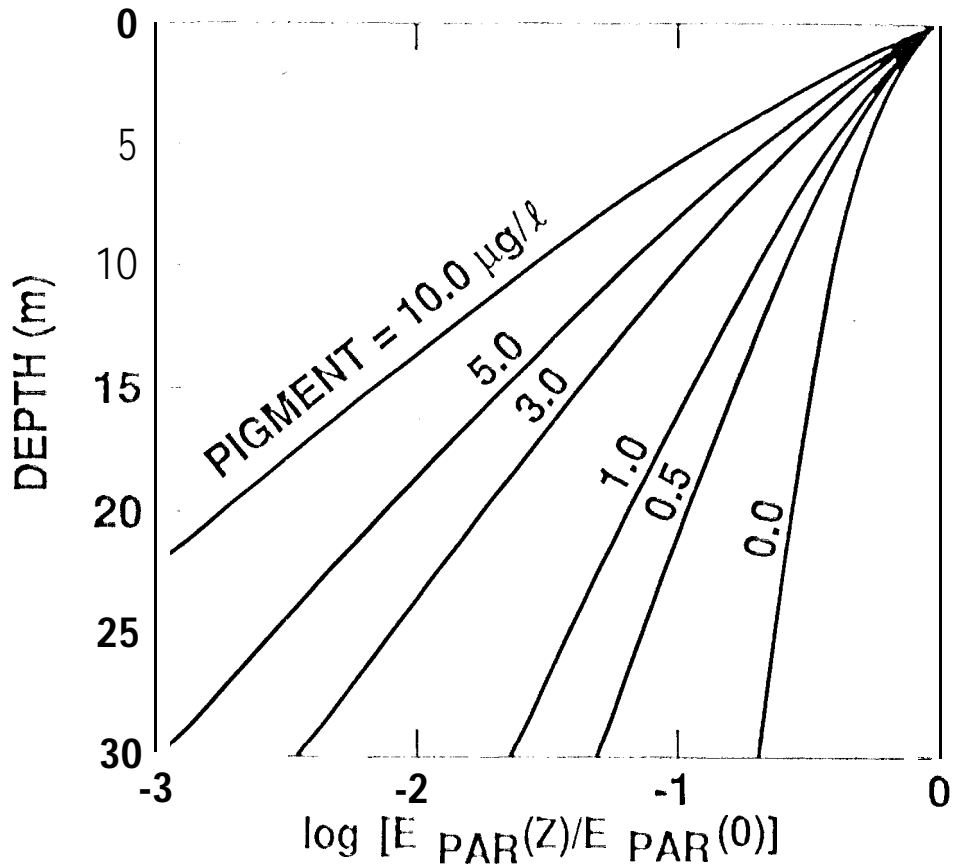
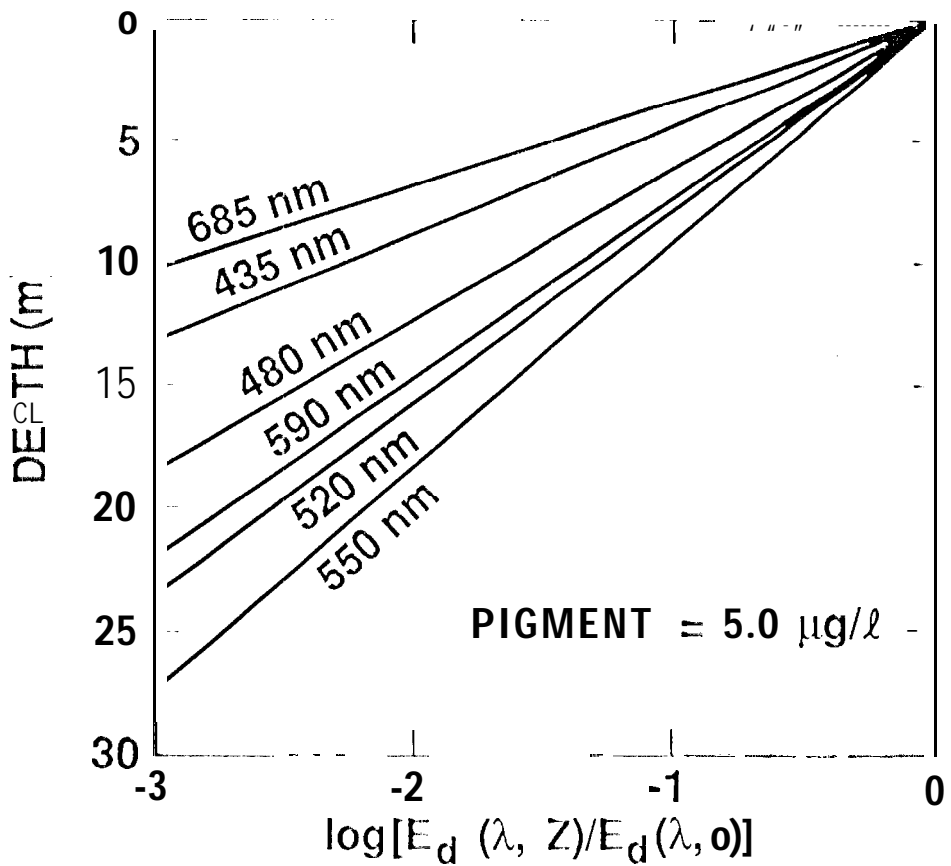


Figure 13





a.  $E_{PAR}$  AS A FUNCTION OF PIGMENT



b. SPECTRAL DISTRIBUTION OF  $E_d(Z)$

Figure 15

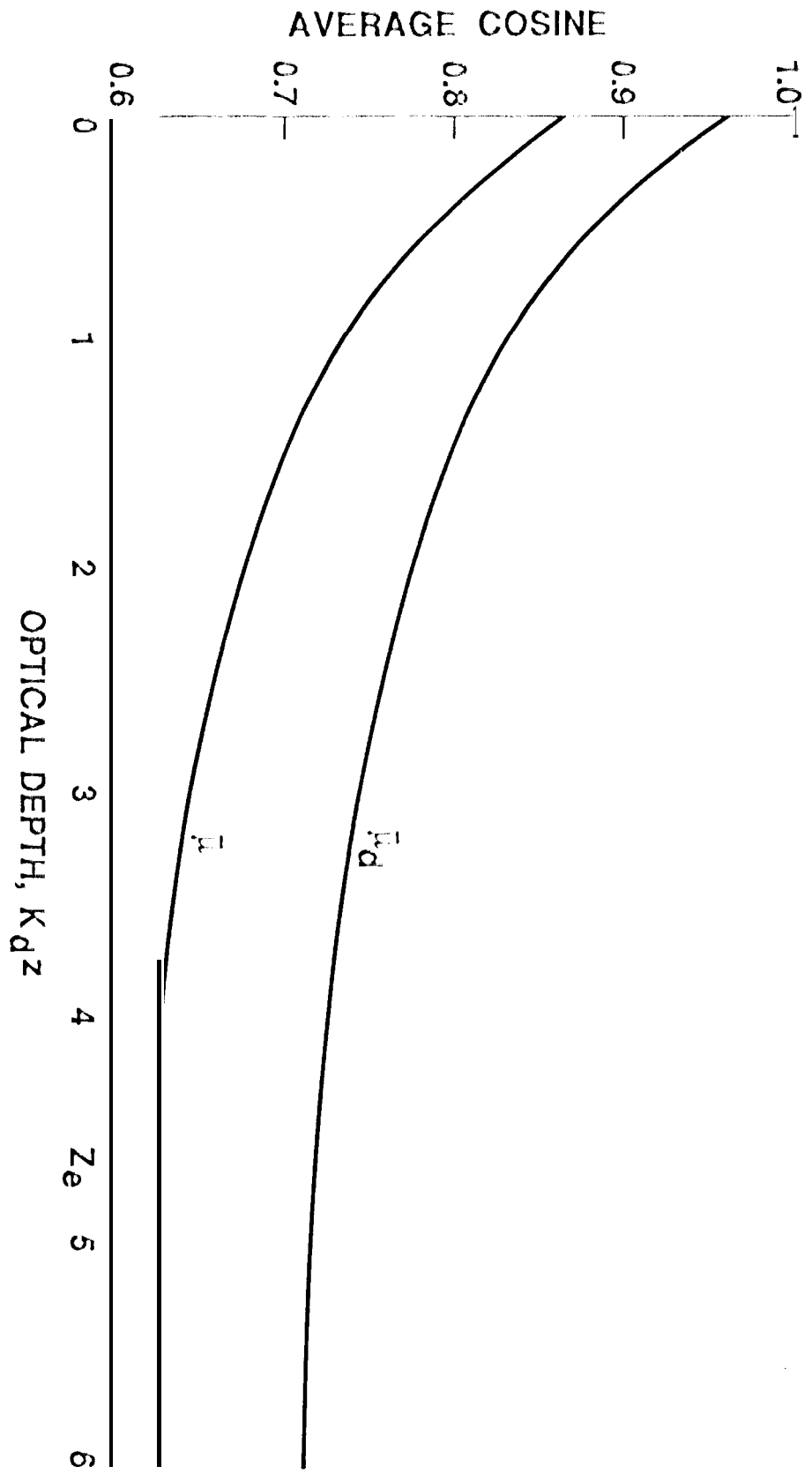


Figure 16

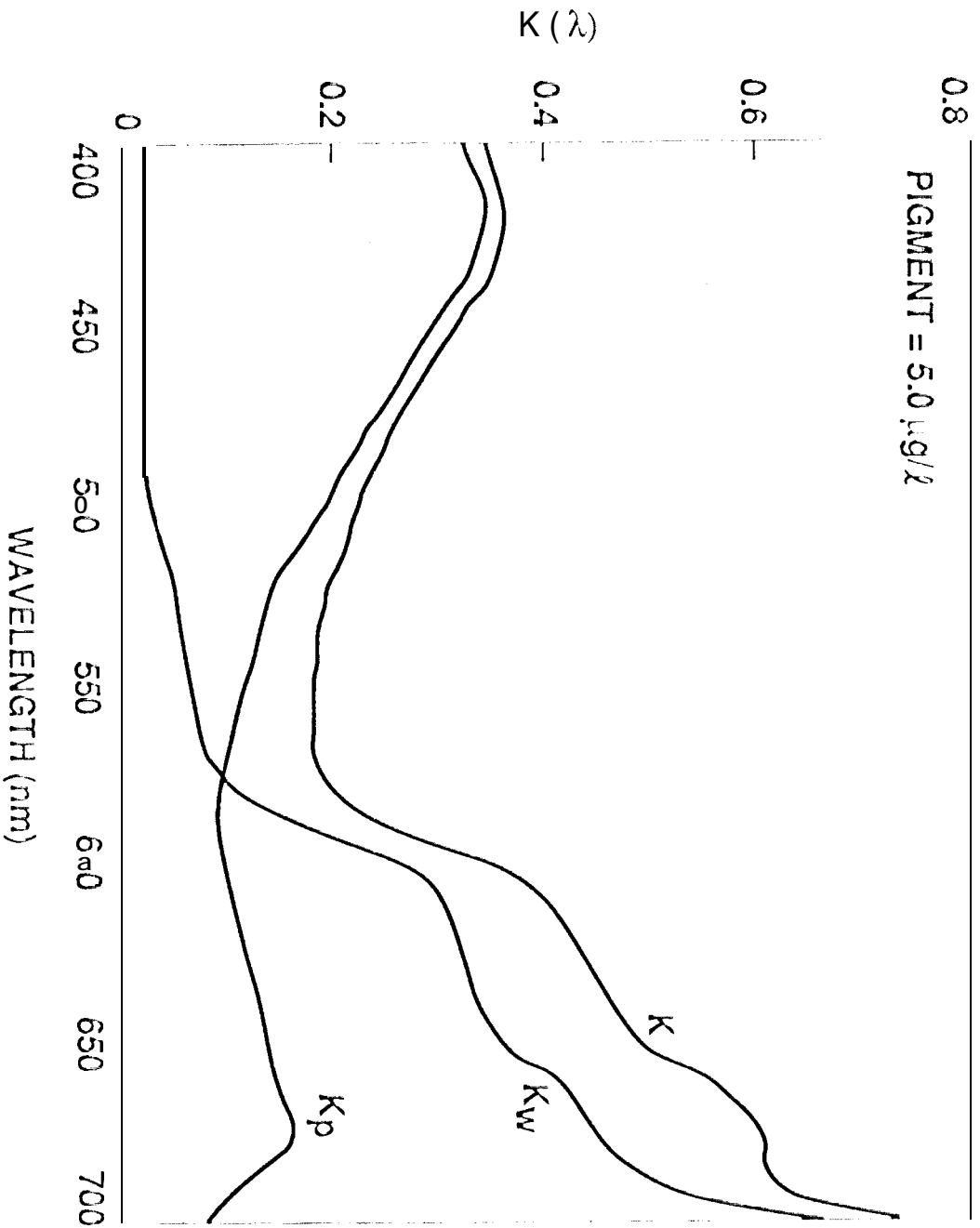


Figure 17

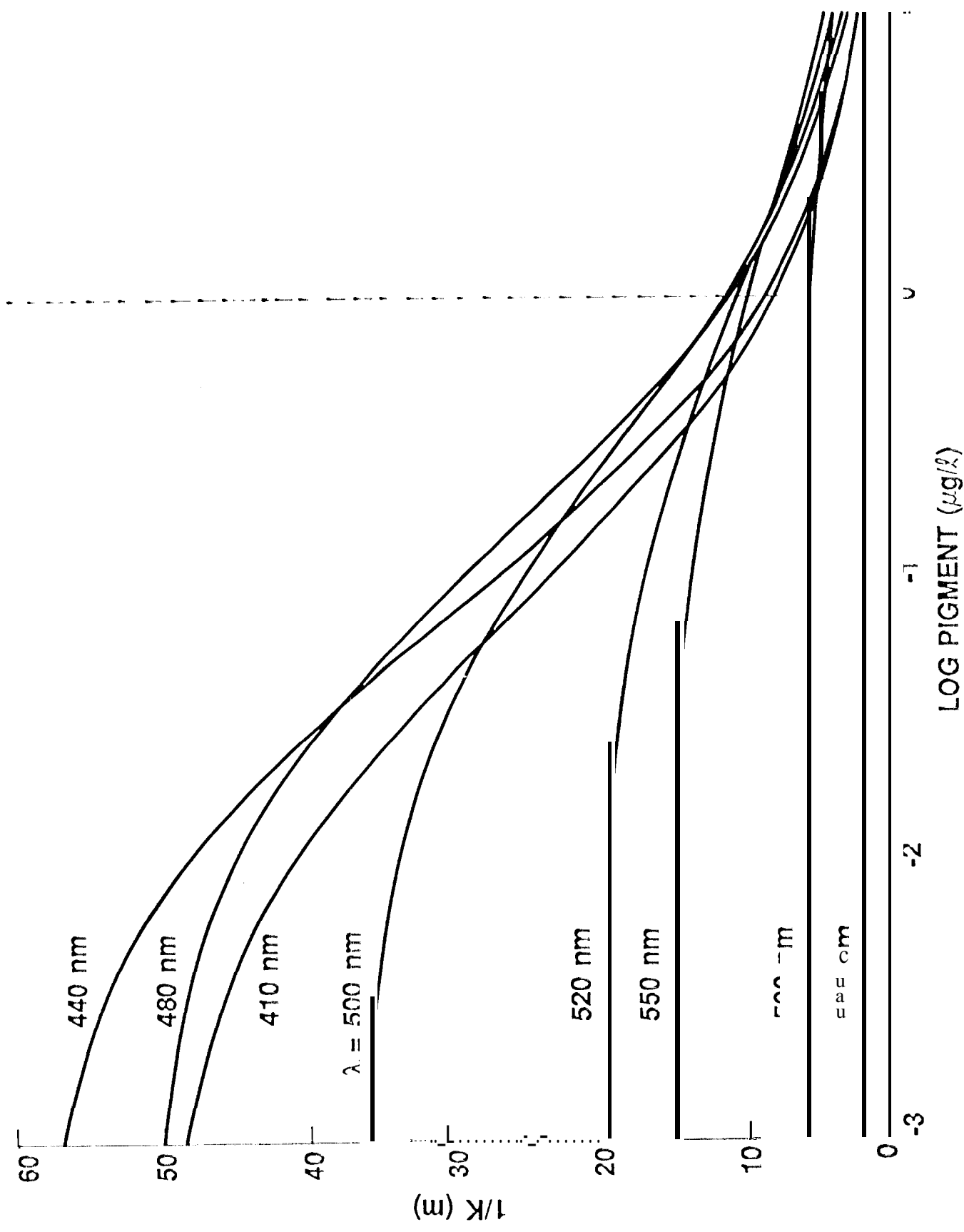


Figure 18

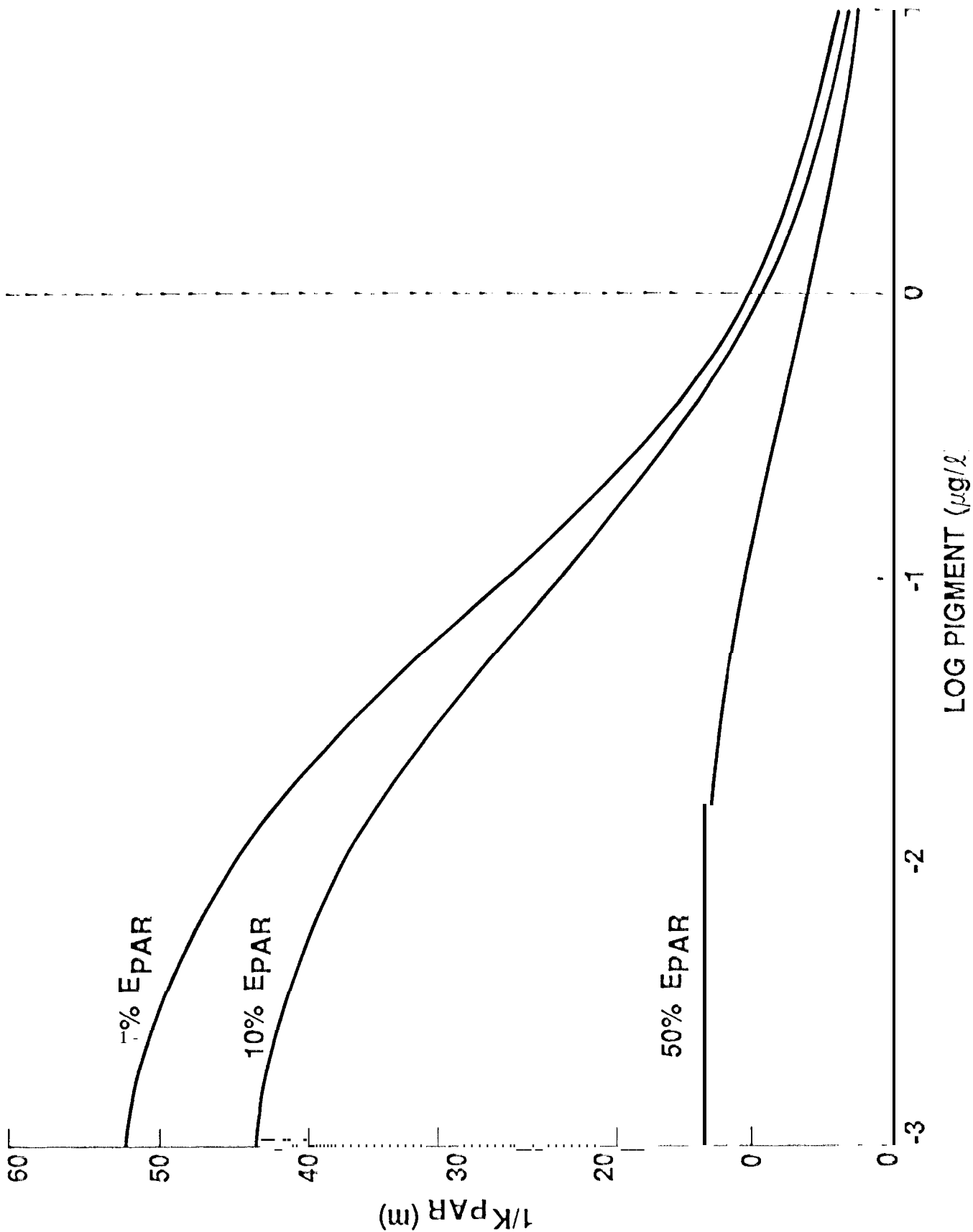


Figure 19

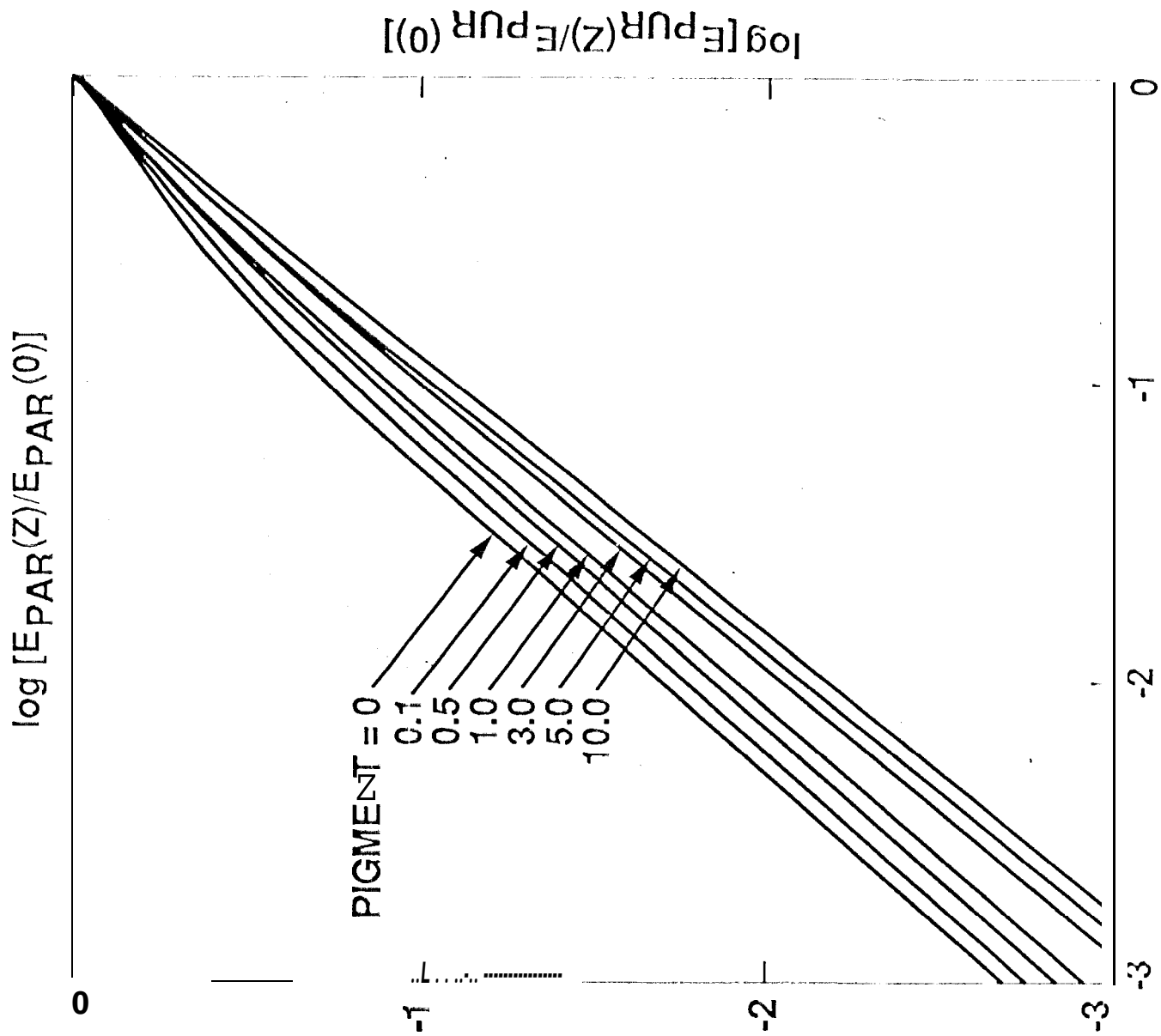
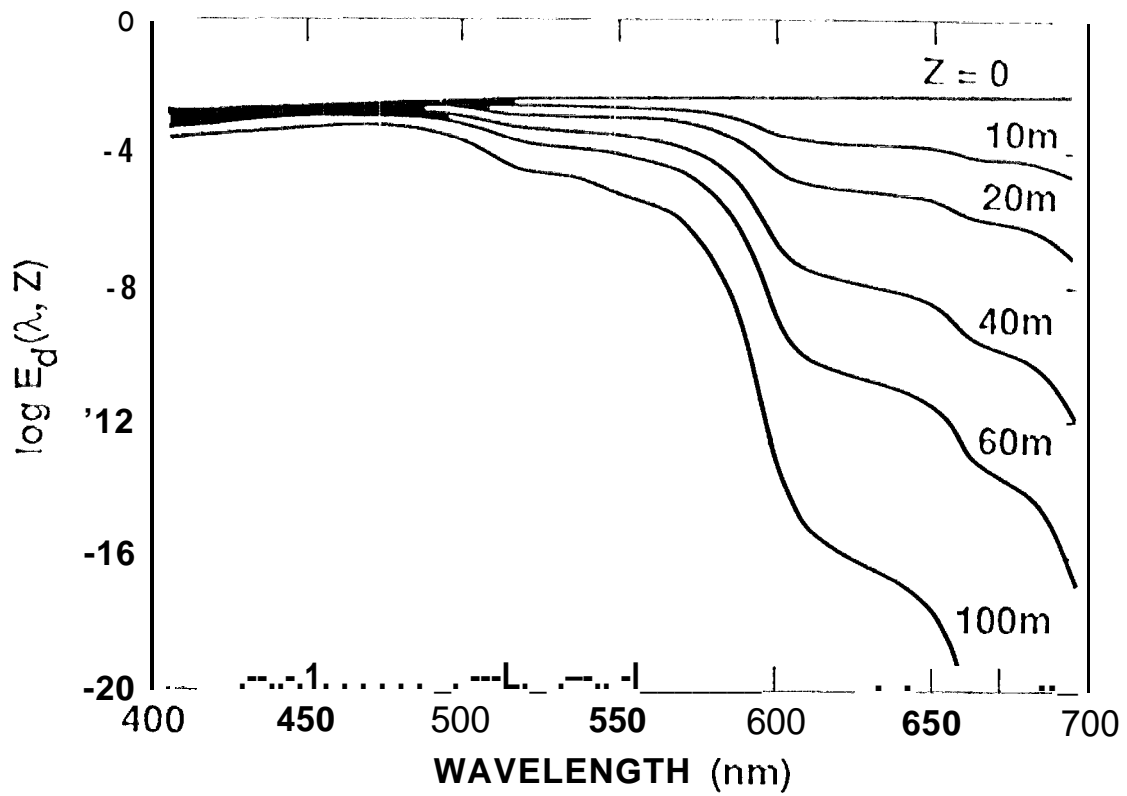
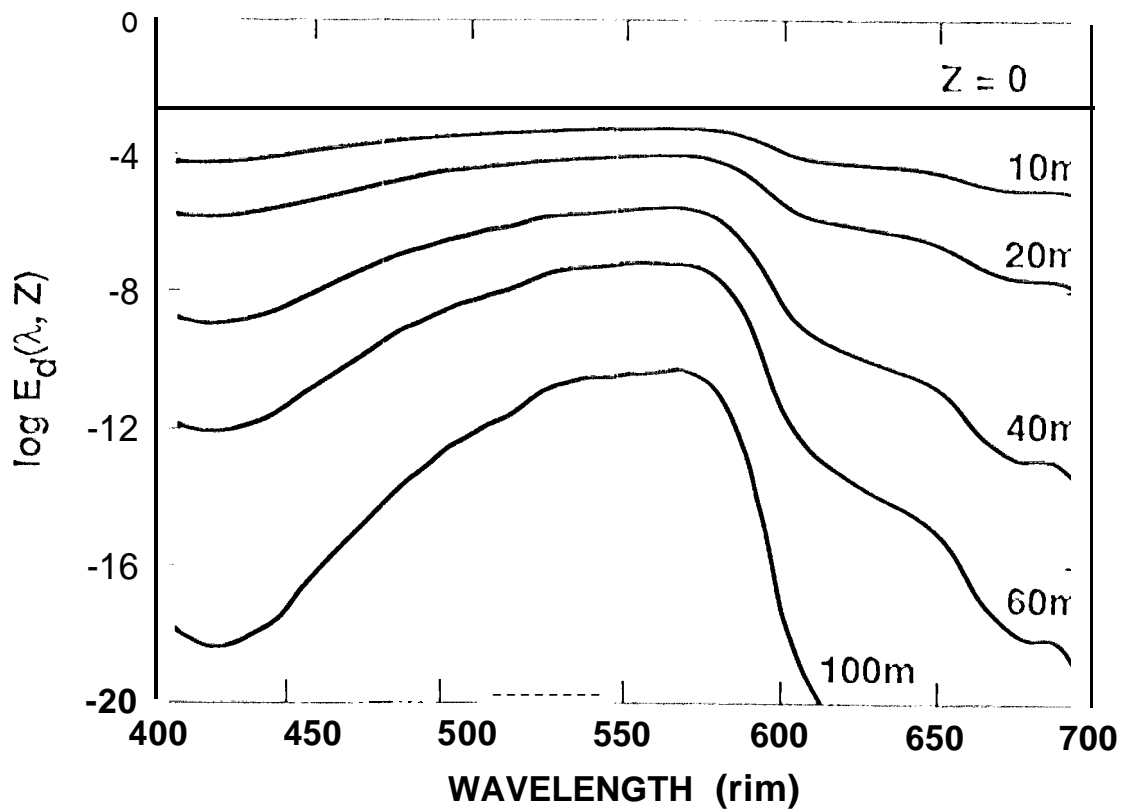


Figure 20



a. PIGMENT = 0.0



b. PIGMENT = 5.0  $\mu\text{g/l}$

Figure 21

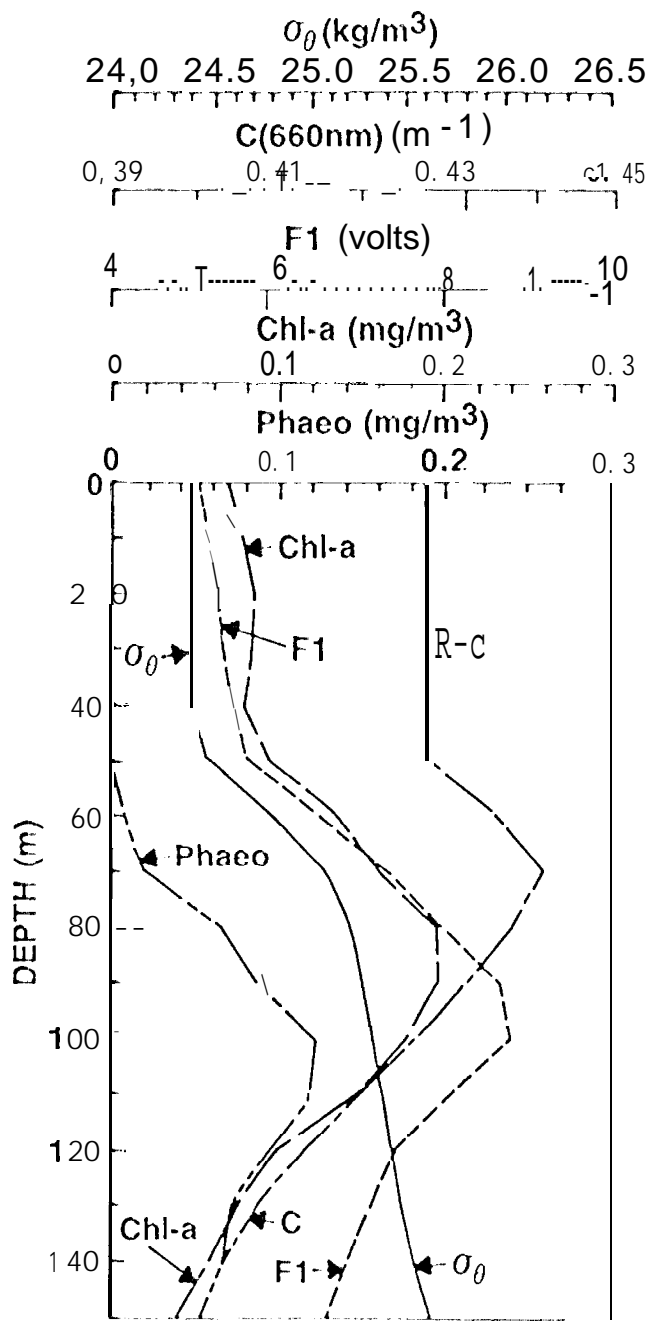


Figure 21a

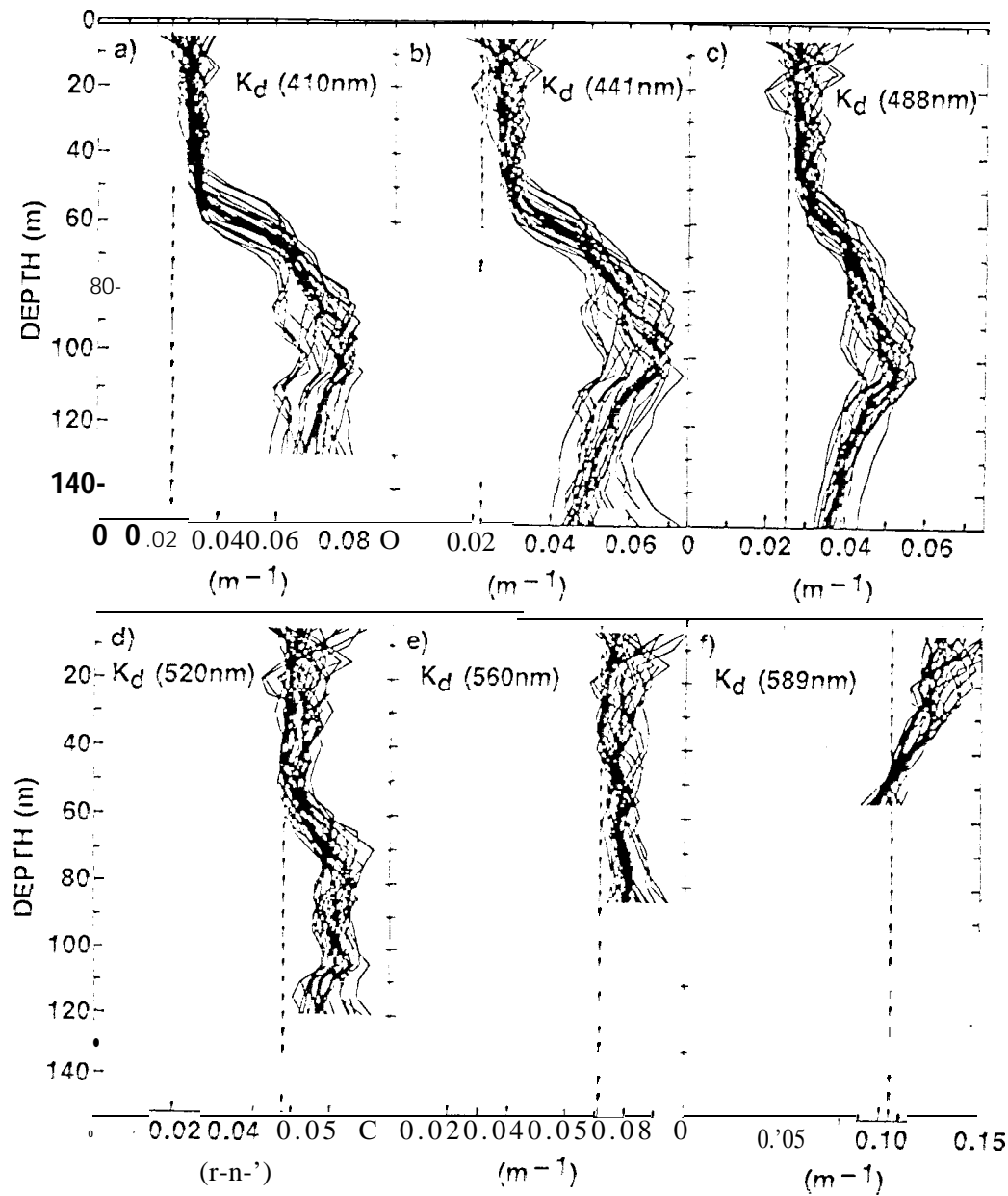


FIGURE 126